



UNIVERSITÀ POLITECNICA DELLE MARCHE

FACOLTÀ DI INGEGNERIA

---

Department of Information Engineering  
Master Degree in Biomedical Engineering

A novel measurement approach for the  
measurement of the diaphragmatic  
contraction by EMG signal

Supervisor:

Prof. Lorenzo Scalise

Candidate:

Laura Ingrassini

Co-Supervisors:

Ing. Luca Antognoli

Prof. Claudio Turchetti

---

Academic year 2018-2019

## Abstract

The study of the biological signals can be essential for discerning the pathological conditions of the human being. Moreover, the investigation of muscle activation, contraction and relaxation are relevant features that provide information about the functionality of the muscle. The evaluation of the muscle activity can be performed by many techniques but the more spread, due to its reduced complexity and invasiveness, is the Surface Electromyography. This non-invasive technique can be applied to the monitoring of the muscles involved in respiration to diagnose pathologies that affect the respiratory system. The diaphragm is the principal muscle involved in respiration, its contraction and relaxation regulate the inspiratory and expiratory phases of the respiratory cycle. In this study, the diaphragm contraction is measured by means of a novel measurement approach based on the employment of adhesive conductive electrodes, made by innovative materials, connected to a wireless device developed by the Electronic group of the Department of Information Engineering of Università Politecnica delle Marche. The coupling between the proposed electrodes and the wireless device has been tested on ten voluntary subjects at which it is asked to alternate five deep and five normal breaths repeated two times. The results prove the ability of this system to detect the diaphragmatic contraction, in particular when it is induced by the deep breaths. Moreover, the system ability showed in the diaphragmatic contraction detection suggests that it could be employed in those patients that require a continuous monitoring of the respiratory system.

## Table of contents

1. Introduction .....	4
1.1 Electromyography .....	5
1.1.1 Diaphragm Electromyography .....	8
1.2 Electrodes for biopotentials recording.....	13
1.2.1 Electrodes materials .....	16
1.3 Aim of the study .....	20
2. Materials and Methods .....	21
2.1 Electrodes developing process .....	21
2.2 Acquisition system.....	24
2.4 Experimental set-up .....	29
2.3 Signal Processing .....	32
3. Results .....	34
4. Discussion.....	55
4.1 Limitation of the study .....	57
5. Conclusion.....	59
6. Acknowledgements .....	60
List of Figures .....	61
Bibliography .....	64

## 1. Introduction

The recording of the biological signals is an important method to evaluate the patient's health conditions. In particular, the measurement of biopotentials coming from the heart, metabolic system or muscles is considered a diagnostic tool for the identification of some pathologies that affect the human body. In fact, the analysis of the electromyographic signals provides information about muscle functionalities in terms of activation, contraction, and relaxation [1]. Electromyography (EMG) is a diagnostic technique that can be applied to different muscles according to the kind of activity that has to be taken under consideration. It can be employed in the evaluation of the locomotion as well as in the evaluation of muscles involved in respiration to identify diseases that affect the respiratory system. By means of the organs that compose the respiratory apparatus are allowed the gas exchanges that guarantee the functionality of the circulatory system. The act of breathing is allowed by the contraction and relaxation of the respiratory muscles. The main muscle involved in this process is the diaphragm, it contracts and relaxes allowing the inspiratory and expiratory phases of the respiratory cycle [1][2]. There are different techniques that can be used to analyse the diaphragmatic motion, from the imaging acquisition modalities to the application of the different EMG recordings that can be divided into invasive or non-invasive approaches. The choice of surface EMG (sEMG) can be preferred to avoid the risks related to the invasiveness of the invasive EMG and, since it is based on the application of surface electrodes in correspondence of the area of interest, it allows the recording of a higher information content due to the presence of a higher number of motor units under the analysed area. Obviously it is very important to choose the diameter of the electrode that reduces the problem related to the cross-talks provoked by the muscle near to the muscle of interest. Usually, the more spread electrodes for biopotentials recording are the Silver Silver-Chloride electrodes [3], the materials by which they are composed allow the collection of biopotentials, but despite their wide range of applications, nowadays different materials are employed in the

biological signals recording with successful results. However, the sEMG not only suffers from the artefacts induced by the choice of the recording electrodes but also by the patient cables that introduce motion artefacts covering the muscle activity. This problem could be dealt with by the adoption of a mobile sEMG system like the one developed by the Electronic group of the Department of the Information Engineering of Università Politecnica delle Marche, this device will be used on the measurement of the diaphragm contraction conducted in this study.

### 1.1 Electromyography

EMG is a diagnostic procedure that allows the analysis of muscle function, evaluating the electrical activity emitted from the muscles [4]. The muscles are composed of individual contractile units known as muscle fibers that are innervated by the axonal terminals of the motor neuron. The basic functional unit of the muscle contraction is the motor unit, constituted by muscle fibers and their related axonal terminal. When the action potential of the motor neuron reaches a depolarization threshold, the muscle fibers contract. The motor unit action potential (MUAP) is the spatial and temporal summation of the individual muscle action potentials for all the fibers of a single motor unit [2]. Therefore, the EMG signal is the algebraic summation of the MUAPs within the pick-up area of the electrode being used. The study of EMG signal allows to detect medical abnormalities, activation level, or recruitment order, or to analyse the biomechanics of human movement.

The EMG signal can be detected using two different approaches, invasive or non-invasive, according to the clinician's necessities [5]. The first solution is based on the insertion of a needle or a thin wire electrode inside the muscle; despite its invasiveness, this technique provides high-quality information on the muscle activation and represents a suitable choice in conditions that require the investigation of neuromuscular disease. Otherwise, the sEMG is the non-invasive procedure used in clinical or physiological researches and in which the overall

activity of a muscle has to be recorded. The sEMG is the procedure adopted in the recording measurement sessions conducted in this study.

In general, the EMG signal is characterized by an amplitude that can range from 0 to 10 mV. The usable energy of the signal is limited to the 0 to 500 Hz frequency range, with the dominant energy being in the 50-150 Hz range. Signals with energy content higher than 500 Hz are related to the noise. There are different factors that can influence the sEMG recording, such as the power line, DC-offset due to the difference in the impedance between skin and electrode, motion artefacts (0-20 Hz) due to the movement of the patient and patient cables connected to the amplifier, Electrocardiography (ECG) artefacts, the nature of the muscles contraction, cross-talks produced by signals coming from other muscles [6]. However, even the patient's anthropometric characteristics can influence the properties related to amplitude, time and frequency of EMG signals [5]. In particular, the electrode placement has to be taken in consideration because a higher distance between the electrode and the investigated area can affect the measurement, losing part of the information content. In addition, the quality of the measurement can be affected even by the skin-electrode interface, for this reason, before the recording, the skin has to be prepared removing body hairs, cleaning and drying it to get a good signal and avoid artefacts.

Although the usage of some preventive measures to reduce artefacts, the collected signal is still characterized by them that can be removed with signal processing techniques. To remove the motion artefacts, the SENIAM protocol recommends high-pass cut-off frequencies of 10-20 Hz. Since the sEMG has an energy content included in the 0-500 Hz frequency range, the suitable low-pass cut-off frequency for the attenuation of the higher frequency components should be around 450-500 Hz, with a sampling frequency of 1000 Hz, according to the Shannon theorem [6] [7].

The modality of EMG acquisition used in this study is bipolar mode. Two recording electrodes should be placed between a motor point and the tendon insertion or between two motor points, and along the longitudinal midline of the muscle. Moreover, a reference electrode is placed as far away as possible and on electrically neutral tissue to provide a common reference to the differential input of the preamplifier in the electrode. In figure 1 is represented the modality by which the electrodes are placed on the interested muscle to measure the biopotentials using two surface electrodes coupled to the skin with electrolytic gel [8].

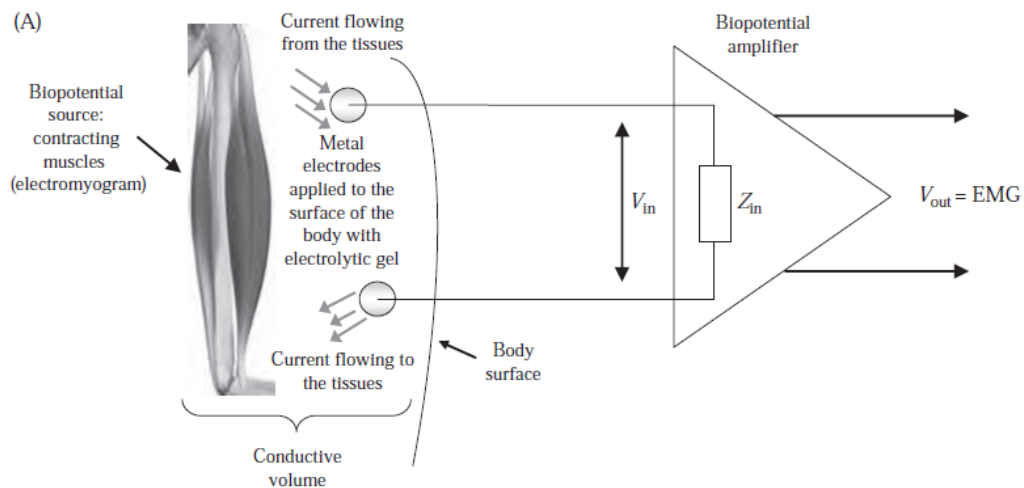


Figure 1 - Bipolar modality sEMG acquisition [7]

The figure below represents the equivalent circuit, in which the depicted left and right branches are the surface electrodes used in the measurement recording [8].

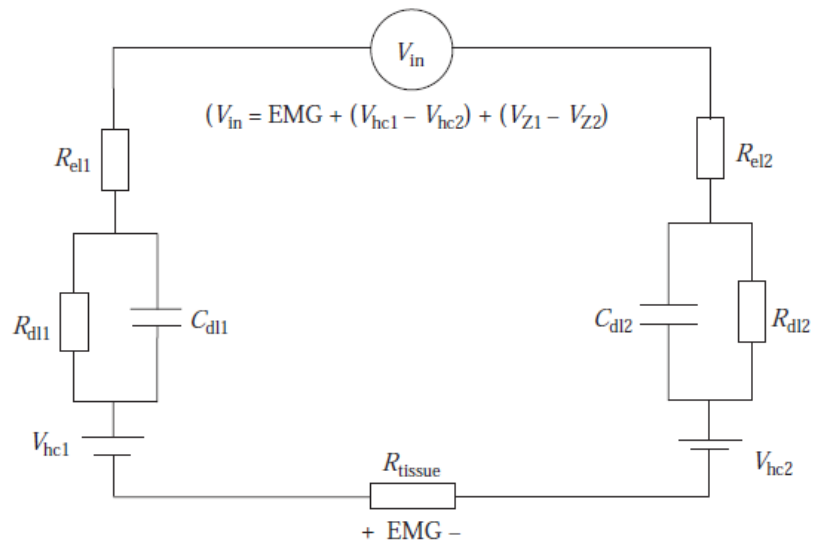


Figure 2 - Bipolar modality sEMG circuital representation [7]

### 1.1.1 Diaphragm Electromyography

sEMG can be applied on different muscles to evaluate muscle fatigue, medical abnormalities, recruitment order, or to analyse the muscle activation level. Moreover, the application of sEMG on respiratory muscles provides information about the functionality of the respiratory system. Although breathing is an automatic activity that the human being executes from the first moments of its life, it is induced by an electrical stimulus in the brainstem that, traveling through motor nerves and the neuromuscular junction, reaches the muscle fibers provoking the muscle contraction.

The respiratory cycle consists of inspiratory and expiratory phases regulated by the contraction and relaxation of the diaphragm [1]. The diaphragm, depicted in figure 3, separates the thoracic cavity from the abdominal cavity, its insertion occurs into the xiphoid process frontally, at the level of the last six intercostal ribs laterally and the first three lumbar vertebrae in the back direction [2]. The diaphragm contraction, followed by its flattening, increases the thoracic cavity volume causing a negative pressure that allows the entrance of air in the lungs during the

inspiration. During the expiratory phase, the diaphragm relaxes coming back to its initial position and removing the air from the lungs [2][9].

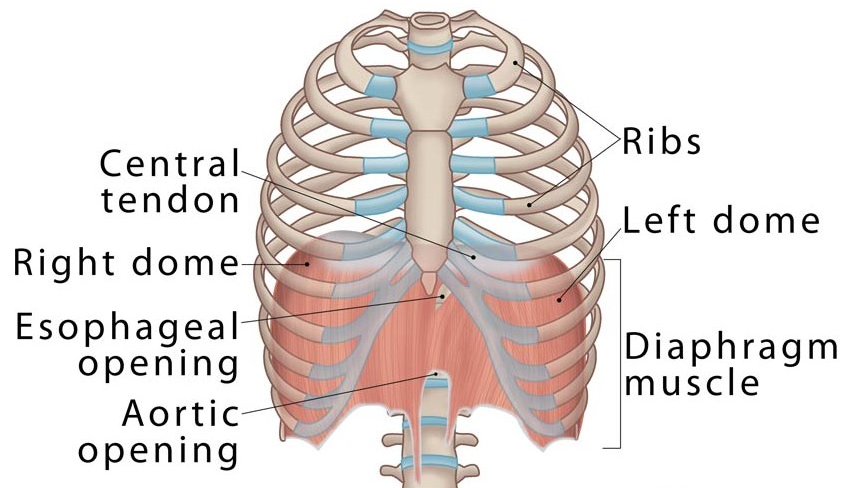


Figure 3 - Diaphragm

There are different modalities to acquire the diaphragmatic EMG signal according to the clinician's judgment and to the patient's clinical situation. First of all, the diaphragmatic EMG signal can be detected in an invasive and non-invasive manner. The invasive solution is based on the positioning of an array of electrodes in the oesophagus to monitor the contraction and relaxation activity of the diaphragm [10]. An alternative to the cumbersomeness of this invasive technique is the diaphragmatic sEMG in which surface electrodes can be positioned on the area of the apposition of the diaphragm to the chest wall. Despite a reduced signal to noise ratio (SNR) respect to the invasive method, the choice of this non-invasive solution gives the advantage to avoid the risk of perforation related to the placement of the electrodes in the oesophagus. However, this advantage is counterbalanced by the presence of a higher number of noise sources such as the intercostal muscles cross-talks, body constitution, and electrode-skin contact interface.

The predominant source of noise that compromises the detection of muscle activation is the ECG signal. Because of the overlap between the frequency content

of the EMG and ECG signals, it is difficult to remove cardiac artefacts from EMG signal. For this reason, the common filtering techniques are non-sufficient for removing the noise source. The combination of traditional filtering technique with enhanced filtering methods is the solution proposed in the study of Alty et al. [11]. In particular, they analyse the diaphragmatic signal using a combination of procedures based on a high-pass and notch filter at 50 Hz, at which follow the Independent Component Analysis (ICA), that allows the separation of multivariate signal into its subcomponents, finally, a low-pass filter is applied to remove the remaining ECG components. After this filtering procedure, the diaphragmatic EMG signal appears to be more clear even if some ECG components are still present. Another appropriate solution to remove the ECG artefacts is represented by the Wavelet Transform (WT), a mathematical tool suitable for the processing of the non-stationary signals. WT decomposes in different frequency components the signal that is made by a set of scaled mother wavelets. Selecting the correct mother wavelet that resembles the ECG signal, WT can be used for denoising purposes, decreasing the ECG content in the EMG signal [12].

The evaluation of the diaphragmatic EMG signal can be useful for the assessment of some diseases, that affecting the respiratory system, could induce an incorrect movement of the rib cage, compromising the pulmonary ventilation. In the systematic review of Masselli et al. [13] are collected different studies in which the EMG is performed on respiratory muscles to assess the respiratory mechanics and muscle functionality. In particular, considering the electrodes positioning and the signal processing techniques is determined if the EMG on respiratory muscles could be suitable for diagnostic purposes. According to the tested respiratory muscles, the electrodes are placed in a specified position. For what concerns the diaphragm, there are some anatomical reference lines that should be used to correctly record the signal, such as the axillary and midclavicular axillary lines. Considering these anatomical landmarks, the recommended positions of the electrodes vary between 5<sup>th</sup> and 10<sup>th</sup> intercostal space but the 7<sup>th</sup> and 8<sup>th</sup> intercostal space are the anatomical parts selected in the most number of the analysed studies, with the

reference electrode placed in the sternum. The acquired EMG signal is then filtered by appropriate filtering techniques, the Root Mean Square (RMS) calculation and frequency domain analysis are the two techniques reported in this study. However, in all of the studies taken under consideration by this systematic review, is demonstrated the reproducibility of EMG on respiratory muscles to assess the functionality of the respiratory system, muscle activation, muscle fatigue and muscle contraction controlled by the nervous system.

A commercially available device to acquire diaphragmatic sEMG and for the monitoring of the respiratory system is Dipha-16, depicted in figure 4. The electrophysiological signal is acquired by a clinician and measured by a reusable sensor and option header, connecting the electrode leads to the patient. The couple of electrodes placed on intercostal muscles, diaphragm muscle, and scalene muscle are attached to Dipha-16 through a multi-connector, the common electrode is placed on the sternum. By means of auxiliary channels, this tool is able to measure the differential pressure (oesophageal and airway pressures). The acquired signal is then transmitted via Bluetooth to the computer, in which it is displayed the six leads, differential pressures, the envelope of the analysed respiratory muscles and Respiratory Rate, Heart Rate and Tacho rate. Dipha-16 contains a DC reference amplifier characterized by low input noise, high input impedance, and high common rejection ratio. Active signal shielding minimizes electrode cable capacitance and therefore cable movement artefacts and sensitivity to mains interference (50/60 Hz). This system is rechargeable by a lithium-polymer battery. Dipha-16 is an appropriate solution for the evaluation of respiratory muscle movement because it can be connected to adult and pediatric patients, but it requires the presence of the clinicians for the patient leads connection and for data interpretation [14].



Figure 4 - Dipher-16 device [14]

The study of the diaphragm movement can be dealt with even imaging techniques such as fluoroscopy. Videofluoroscopy provides information about the distance reached by the diaphragmatic excursion during respiration evaluating the muscle motility. This approach is very useful to evaluate the weakness of the diaphragm in pathological patients and after surgical interventions, in presence of malformation and the muscle contraction. The ability to detect the left and right displacement of the diaphragmatic muscle makes the videofluoroscopy a reliable tool for the measurement of the diaphragmatic excursion, even if it depends on the clinician's evaluations and it submits the patient to the radiations [15].

iMEMS acceleration sensor represents a good alternative to avoid the risk related to radiation exposure in videofluoroscopy. The iMEMS, made of a silicon chip that consists of micromechanical structures and electrical circuits, acquires, measures and records the muscle movement. The acceleration sensor is ADXL345, that senses the acceleration in three directions with the z-axis directed perpendicular to the diaphragm. The circuit of the system includes PIC16F88 microcontroller, 2x8 character LCD display, accelerometer sensor, eeprom memory component, and data transfer circuit card. Moreover, the measurement conducted on five patients demonstrates that this device, compared to the spirometer, enables to diagnose respiratory disease by the monitoring of diaphragm activity [16].

## 1.2 Electrodes for biopotentials recording

The measurement of the biopotentials involves the electrode, a device that works as an interface allowing the passage of current from the human body to the measurement system. In particular, at the skin-electrode interface occurs the conversion of ionic current, which characterizes the biological tissue, into electrical current to make possible the recording of the physiological signal.

The recording of muscle activity during sEMG depends on the geometry and material that characterize the electrode. Moreover, the surface electrodes can have fixed or variable geometry according to the recorded muscle activity. For example, smaller dimensions of the electrodes can be recommended to reduce the cross-talks produced by EMG signals coming from other muscles than the ones being monitored. Albeit a smaller dimension has the advantage to decrease some noise sources, because of the strict dependence between the electrode dimension and electrode impedance, a reduced electrode dimension provokes an increase in the electrode impedance. In fact, the size of the electrodes plays a very important role in the evaluation of the impedance, because the smaller the electrode dimension, the higher the impedance. However, the non-polarizability and the higher SNR make the silver silver-chloride (Ag|AgCl) electrodes the more spread in the medical applications, because of the materials that compose them, it is possible the realization of chemical reactions that allow the conversion of the ionic current into the electrical current at the skin-electrode interface depicted in figure 5.

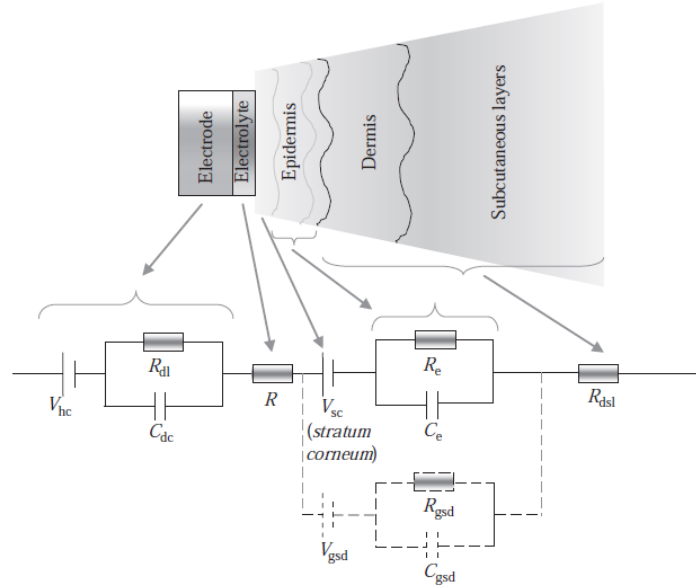
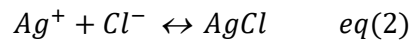
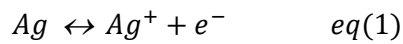


Figure 5- Electrode-skin interface [8]

The presence of AgCl favours the chemical reaction in the electrolyte-skin interface, allowing the flow of ionic and electric current in the skin and electrode respectively. In particular, the signal collected by the electrode applied on the skin is made of a weak ionic current, that has to be transformed into an electrical current to be compatible with the electrical current that flows in the conductors that send the signal to the measurement device. To allow this transformation is necessary that the electrode is constituted by metal in contact with its saline solution in which can occurs the chemical reactions. The chemical reactions that occurs at the electrode-electrolyte interface are the following:



The first represents the oxidation of the Ag ions into  $Ag^+$  ions, which occurs when the silver electrode is coupled with the silver chloride solution, allowing the transfer of electrons to the silver electrode. Since the products of the chemical reaction are  $Ag^+$  ions, the electrolytic solution shows a higher concentration of positive charges,

leaving the silver electrode to become negatively charged due to the flow of electrons on it. By means of the flow of charges, there is the development of a potential difference. Moreover, it is important to take into account that the reaction takes place only when the silver electrode makes contact with the silver chloride solution reaching the equilibrium determined by a potential difference of 0.7791 V.

The second reaction takes place only when the first occurred because it requires the formation of  $\text{Ag}^+$  ions, that are combined with  $\text{Cl}^-$  to create  $\text{AgCl}$ . The main characteristic of the  $\text{AgCl}$  chemical compound is to be very slightly soluble in water, making possible to increase the deposit of silver chloride on the silver electrode.

The presence of a double layer of charges, due to the occurred chemical reactions, causes the electrode to behave like a condenser, in which the impedance varies with the frequency, in fact, it decreases linearly with the frequency, showing a lower value of impedance at a higher value of frequencies [8].

In addition, it is necessary to take into account the resistance that the ionic and electrical conductors, represented by the skin and the electrode respectively, oppose to the passage of the current. Considering this concept is possible to give to the electrode a circuitual interpretation depicted in the following figure 6.

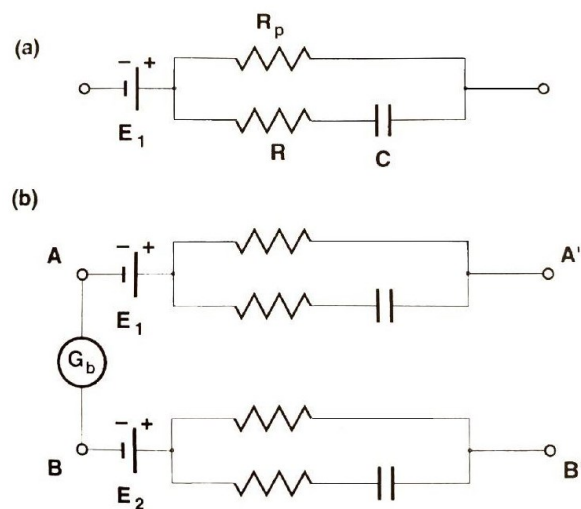


Figure 6 - Electrode circuitual representation [17]

The first circuit (Figure 6 a) consists of a resistance  $R$ , that is the electrode resistance opposed to the passage of the current, the electrode capacity  $C$ , the resistance indicated with  $R_p$  is required to consider that the current flow in the electrode also when the frequency is equal to zero and  $E_1$  is the generator of the potential difference produced by the double layer of charges.

The potential difference is recorded when two electrodes are applied to the conductive tissue, for this reason, it is necessary to consider the second circuit (figure 6 b) that is obtained considering the employment of another electrode. In this circuit,  $G_b$  represents the generator that considers the capacity and the resistance of the tissue between the two electrodes,  $E_1$  and  $E_2$  are the two electrodes generator. Since the two generators are placed in an opposite position in the circuit, their contribute is null to  $A'$  and  $B'$ . The potential difference that is present between  $A$  and  $B$  is available also in  $A'$  and  $B'$  and this can be useful for the measurement of the potential difference [17].

### 1.2.1 Electrodes materials

The study of Tallgre et al. [3] proves that the electrodes realized in  $Ag|AgCl$ , compared to other types of material such as gold, platinum, and stainless steel, shows the better characteristics in terms of offset voltage, resistance, polarization, and noise level, this is a demonstration of the ability of  $Ag|AgCl$  electrodes to collect the biological signals.

Despite the success that the  $Ag|AgCl$  electrodes shown in the measurement of biopotentials, nowadays different materials can be taken into account for the electrodes realization.

The materials involved in the production of the electrodes have to be selected following all the requirements given by the biocompatibility to not damage the tissue. Moreover, the biocompatibility refers to the reaction that the tissue has in contact with the material, then, since the electrodes have to provoke a biological

response, the material with which they are composed have to be appropriate for the interaction with the skin [1]. For this reason, it is necessary to control the presence of deleterious substances that could produce dangerous effects provoking undesirable reactions on the skin.

In the most number of the analysed studies, the base of the electrodes developing process is represented by the electrode 3D printing, the selected material is usually the polylactic acid (PLA). The 3D printing procedure is then followed by a coating process, in which the 3D printed structure is coated with conductive materials. The study of Krachnov et al. [18] proposes two types of electrodes obtained from two different developing processes. In the first approach, the electrode is 3D printed in plastic and carbon-based conductive compound to give intrinsic conductive properties to the electrode. The conductive properties of the carbon-based conductive compound let to avoid the coating process that is instead performed in the second approach. In the second solution, the 3D printed structure is realized with plastic material and then, the conductive properties are given by the coating process in which the plastic material is coated with a conductive compound. The functionality of the obtained electrodes is tested compared to the reference ones, the Ag|AgCl, in the analysis of electroencephalography (EEG). Since the 3D printed electrodes are involved in the evaluation of EEG signal, they are designed with long and thin prongs, as shown in figure 7, penetrating the hairs to achieve contact with the skin. However, the analysis of EEG signal demonstrates that the proposed electrodes are able to detect the waveforms that characterize the EEG tracing, proving the reliability of the proposed electrodes compared to the reference ones.



Figure 7 - Electrode prototype, PLA 3D Printing, Coating process [18]

A similar approach is proposed in the study of Wolterink et al. [19] in which the electrodes, depicted in figure 8, are realized by a process of fused deposition modeling, melting a thermoplastic filament and depositing the material layer by layer. In particular, the selected material for the realization process is filament thermoplastic polyurethane (TPU), particles of copper or conductive carbon are mixed to allow electrode conductivity. In this study, the produced electrodes are compared to the reference Ag|AgCl in the evaluation of the muscle contraction by EMG. Moreover, the comparison between the innovative electrodes and the reference ones proves the validity of 3D printed electrodes in the evaluation of the EMG signal.



Figure 8 - 3D Printed Electrode [19]

In the study of Salvo et al. [20] the evaluation of EEG and ECG is performed comparing dry and wet electrodes. The dry electrode support is realized using an insulating transparent biocompatible acrylic-based resin, FullCure 720, that is submitted to a metallization process organized in two consecutive steps: in the first

step a layer of titanium is sputtered to facilitate adhesion, in the second step a gold layer is evaporated to lower the impedance and prevent corrosion and oxidation. The 3D printed electrodes, depicted in figure 9, have higher impedance respect to the wet electrodes, but the evaluation of ECG and EEG confirm the validity of dry electrodes compared to the reference ones.

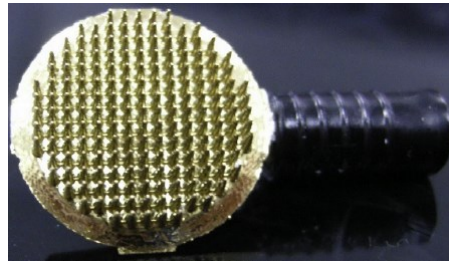


Figure 9 - Dry electrode [20]

The application of these materials in the realization of dry electrodes takes place in different fields that not only involve the measurement of electric biopotentials but also in the development of wearable pressure sensors, wearable temperature-humidity sensors, wearable electrochemical sensors and for healthcare monitoring sensors. All of these application fields are described in the study of Wang et al. [21] in which the conductivity of the electrode is provided by the employment of advanced carbon materials. The good electrical conductivity, high chemical and thermal stability, low toxicity and the functionality make the advanced carbon materials an optimal solution for the development of wearable electronics sensors. In addition, these characteristics make the advanced carbon, the suitable material in the development of wearable sensors that have to monitor electrophysiological signals (EEG, ECG, EMG) reducing the electrode-skin interface's impedance and facilitating a better adhesion between the electrode and the skin allowing the biological signal recording during physical activity.

### 1.3 Aim of the study

The aim of the conducted study is to develop a novel measurement approach for the measurement of the diaphragm contraction, evaluating the functionality of the produced electrodes in terms of conductivity and detectability of the diaphragm sEMG investigating the diaphragmatic movement produced by deep and normal breaths using the device developed by the Electronic Group of the Department of Information Engineering of Università Politecnica delle Marche.

## 2. Materials and Methods

In the following sections are described the developing process for the realization of the electrodes and the data acquisition.

### 2.1 Electrodes developing process

The electrodes developing process involve the design of a prototype, on appropriate CAD software, to standardize the shape of the electrodes. Moreover, the designed prototype is then 3D printed in PLA and is used as support for the electrodes realization. The PLA-3D printed support is then placed on an adhesive gel patch, depicted in figure 10, that is commonly used in the electromagnetic simulation. The adhesive gel patch is primarily composed of the hydrogel. The 3D structure of hydrogel, composed of hydrophilic groups contained in synthetic or natural polymers, makes this component permeable allowing the absorption and containment of a relevant amount of water. When this chemical compound enters in contact with the water, the presence of hydrophilic groups allows the formation of a water bond that can be destroyed in the case of hydrolysis [22]. A fundamental requirement that the hydrogel should have is biocompatibility, this is guaranteed by the presence of hydrophilic groups that create a low interfacial free energy surface when interact with fluid. In fact, the hydrogel biocompatibility avoids damaging the tissue allowing the safe collection of the biological signal [1]. In addition, thanks to the elasticity and flexibility of hydrogel, the adhesive gel patch can fit perfectly the skin and for this reason, is an appropriate base in which deposit the electric paint for the recording of electrophysiological signals.

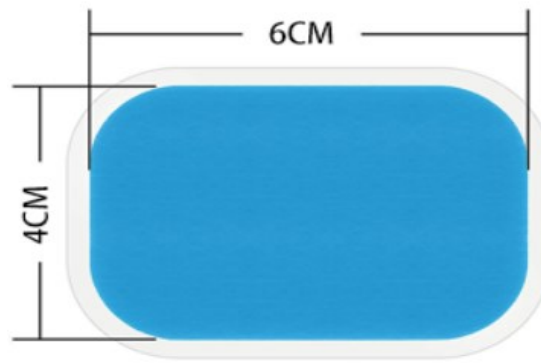


Figure 10 - Adhesive gel patch

The materials by which the gel patch is composed are not able to conduct the body ionic current, for this reason, it is necessary to give it a conductive coat, allowing the conductivity of the biological signal. This requirement is provided by the deposition of conductive material on the surface of the adhesive gel patch. The selected conductive material is the Bare Conductive Electric Paint (fig 11) [23]. The ingredients that compose this conductive paint are water, natural resin, conductive carbon, humectant and processing aids, and preservatives. The presence of conductive carbon on the conductive ink makes the adhesive gel patch able to conduct the electrical signal coming from the area in which the electrode is placed. The conductive ink is deposited between the protective film and the surface of the adhesive gel patch to avoid the direct contact with the skin, even if the interaction of this electrical paint with the skin is not dangerous because of the properties of its ingredients.



Figure 11 - Bare Conductive Electric Paint [23]

The main characteristics of the Bare Conductive Electric Paint are reported in Table 1.

Table 1 – Bare Conductive Electric Paint characteristics

Appearance	Liquid
Colour	Black
Odour	Slight
pH (value)	5-7
Melting Point	Approx-10degC
Evaporation rate (Water=1)	1
Density (g/ml)	1.2-1.25 at 25 degC
Solubility (Water)	Partially soluble
Solubility (Other)	Partially soluble in organic solvents
Viscosity	Viscous liquid

Then, it is placed a graphene conductive strip between the protective film and adhesive gel patch in which the conductive paint has been deposited. In the following figure (fig. 12) is depicted the obtained adhesive conductive electrode realized following the steps described in the developing process.



Figure 12 - Adhesive conductive electrode

The electrodes are then placed on the interested muscle to record and monitor its electrical activity. In the figure below is shown the electrode-skin interface.

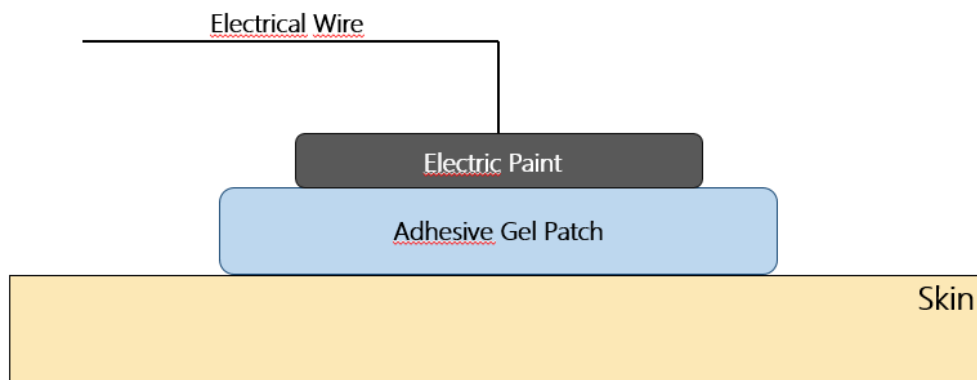


Figure 13 - Adhesive conductive electrode-skin interface

## 2.2 Acquisition system

The acquisition system by which the sEMG measurements are conducted is developed by the Electronic Group of the Department of Information Engineering of Università Politecnica delle Marche. Actually, this system represents an update of an existing wireless device developed for the recording of cardiac and muscular signals, called WiSE [24]. The acquisition, digitalization, and amplification of the electrophysiological signals in WiSE device occur by means of wireless sensing mobile node that transmits the collected signals to more than one base station by 2.4 GHz radio link thanks to a customized communication protocol designed following the IEEE 802.15.4 physical layer. The signal is then sent to a control PC by

a USB link. However, the functionality of the system is guaranteed by the components of the mobile node: AC-coupled instrumentation amplifier, a programmable gain amplifier, a circuit for common mode biasing and an electrode contact resistance measurement, a low pass filter, a power supply circuit, a 3-axis accelerometer, and an 8-bit microcontroller. The components of the current version of the WiSE device are completely different. In particular, the current version consists of nRF52840 [25] to support Bluetooth Low Energy (LE) communications, in order to allow the connection between the mobile node and the computer that in real-time elaborate the collected data. The acquisition of the EMG signal occurs through the ADS1293 [26], an electrical amplifier that is able to acquire the ECG and EMG signal even during sportive activities. Finally, the electrical component LSM6DSO [27] represents the inertial platform for the recording of gyroscope and accelerometer signals. The power supply is guaranteed by a lithium-polymer battery charger that has a maximal duration of two days, allowing the recording of the electrical activity without the possibility of a discharge of the system, avoiding the loss of the acquired data. Moreover, the presence of switching arrays improves the duration of the battery, switching off the components that are not necessary during the acquisition session and allowing a reduction of power consumption. The following figure (fig. 14) shows the block-scheme of the mobile sEMG device.

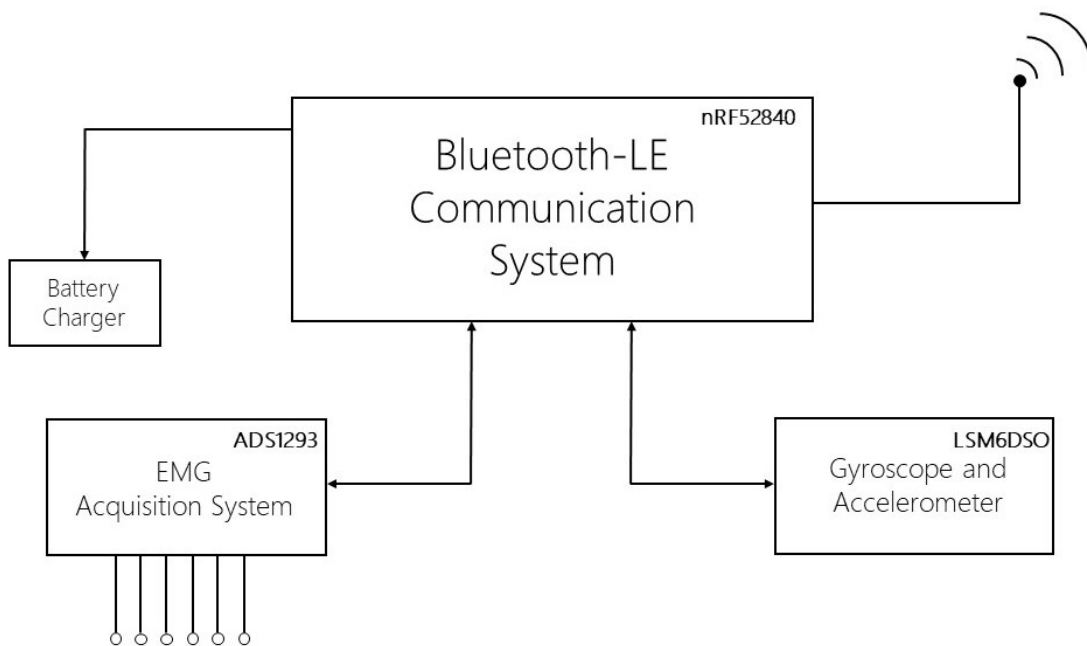


Figure 14 - Mobile node block-scheme

The communications between the control computer and the electronic device occur by a Bluetooth-LE system. The Bluetooth-LE provides the information content to the control computer through a very low power, flexible chip, the nRF52840 Multi-Protocol System-on-Chip (SoC), that is the most advanced member of the nRF52 Series SoC family. It has a dimension of 7 mm x 7 mm and it is a suitable choice for short-range data transmission. In fact, it has protocol support for 802.15.4 radio link, Bluetooth mesh, Thread, Zigbee and Bluetooth 5's Long Range feature. This latter improves the performance capabilities and allows a longer range of data transmission and throughput modes. The characteristics whose this electronic component consists make it an appropriate solution for home networking protocols. The power voltage has a range of variation of 1.7 V to 5.5 V, it is supplied by a rechargeable battery and USB supply without the need for the external regulators. Furthermore, the nRF52840 is composed of many peripheral components powered by an independent and automatic clock and power management that switch-off the single component when is not necessary to save power consumption. The advantage of this electronic component is that it can be employed in different fields, from the industry to healthcare such as smart home

products, smart city infrastructures, fitness devices, virtual and augmented reality and gaming controller.

The ADS1293 is the electronic chip used for the biopotentials recording. It has a dimension of 5 mm x 5 mm and it can be used to monitor ECG during lower-medical activities, sports, and fitness. In particular, in this study, it is used to measure the ECG and EMG signals. The amplifier contains three high-resolution channels that can be independently programmed for customized sampling rate and bandwidth to allow the users specifications. The possibility to give to each independent channel customized properties allows an optimized performance. The advantage of the ADS1293 is represented by reduced size, power and costs and by the presence of a self-diagnostic alarm system that works to detect the on and off time of activations. The ADS1293 can be used in portable 1-12-Lead ECG, patient monitoring, telemedicine, automated external defibrillator and in the monitoring of vital parameters during sport and fitness activities.

The measure of the gyroscope and accelerometer is provided by an inertial platform, the LSM6DSO, 2.5 mm x 3 mm x 0.83 mm of dimensions. The LSM6DSO packaging consists of 3D accelerometer and 3D gyroscope, in fact, it detects the gyroscopic information and the acceleration by means of a frame system organized in 6 axes of motion, the 3-axis for the digital accelerometer, and 3-axis for the digital gyroscope. In addition, it provides high-performance mode at 0.55 mA and enabling always-on low-power features for an optimal motion experience for the consumer. Because of its robustness, due to the plastic land grid array package, it can be employed in many manufacturing processes offering ultra-compact solutions. In order to avoid power consumption, it is provided by a tilt function that activates the system by a user tilt. It finds applications in the development of sensor hub, indoor navigation, motion tracking, and gesture detection, vibration monitoring and compensation.

The power supply of the system is a lithium-polymer battery charger and a cluster of linear and switching regulators to provide power only when the components of the system have to be activated.

The following picture (fig. 15) represents how the analysed components are assembled on the electrical base and the connection to the lithium-polymer battery that supplies the power to the electronic system.



Figure 15 - Mobile node composition

In the following figure (fig. 16) is highlighted the architecture of the base station.

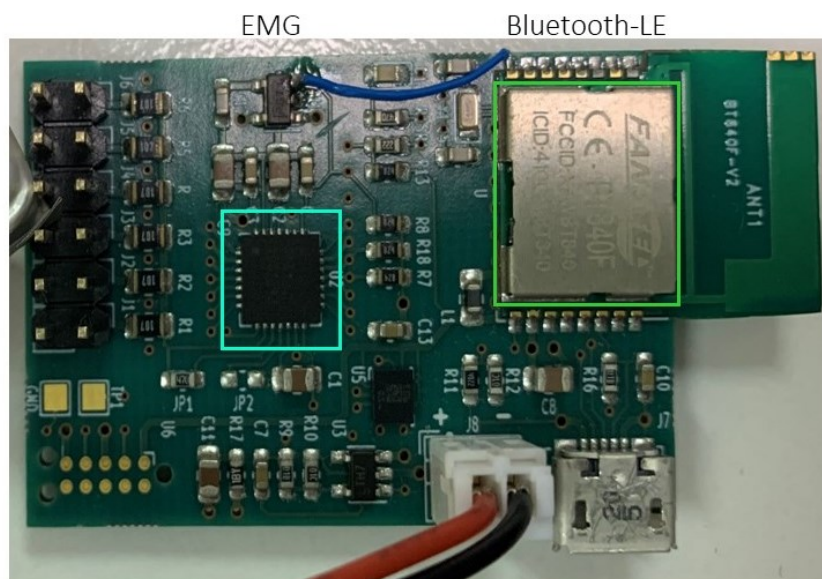


Figure 16 - Mobile node architecture

In the following table are listed the device features.

Table 2 – Mobile system characteristics

Resolution	24 bit
Sampling Frequency	800 Hz
EMG channels	3
Autonomy	2 Days
Dimensions	26.7 mm x 42 mm
ECG	Yes
Accelerometer	Yes
Gyroscope	Yes

## 2.4 Experimental set-up

The aim of the experimental session is to test if the produced adhesive conductive electrodes and the wireless system are able to detect the diaphragm motion induced by deep and normal breaths performed by adult voluntary subjects. Before to start the recording sessions the participants sign a written consent in which are explained the risks, the aim of the project and the measurement protocol.

The measurement protocol is based on the alternation of five deep and five normal breaths repeated in two recording sessions. The diaphragm contraction detected by the adhesive conductive electrodes is firstly measured on the AD Instruments PowerLab 4/25T (fig. tot), then on Dipa-16 Device and finally on the system developed by the Electronic group. In particular, the measure performed with AD Instruments PowerLab 4/25T, an instrumentation amplifier that consists of two

isolated biological inputs (with common ground), constant-current isolated stimulator output, two non-isolated analogue inputs, two analogue outputs, two Pod inputs and trigger input, has the utility to evaluate the correlation between the diaphragm contraction and relaxation related to the inspiratory and expiratory phases detected by the spirometer (fig. 17), a measuring device for the assessment of the respiratory rate using a differential pressure transducer. The signal is acquired using LabChart software selecting the appropriate range and filtering values.



Figure 17 – Spirometer

Moreover, the produced electrodes are tested using the Dipa-16 Device, in which it is used only the couple of the electrodes involved in the measurement of the diaphragmatic activity respect to the other two couples used for the scalene and intercostal muscle. The signal is then transmitted by USB-Bluetooth connection to Polybench Data Manager software on the control computer to have a real-time visualization of the data recorded.

Finally, the customized electrodes are connected to the mobile node developed by the Electronic group to starts the campaign of measures to evaluate the ability of the produced adhesive conductive electrodes and the mobile device to measure the diaphragm contraction in different subjects with different anthropometric characteristics.

The table below indicates the anthropometric characteristics of the subjects involved in the study.

Table 3 – Anthropometric characteristics of voluntary subjects

<b>ID</b>	<b>SEX</b>	<b>AGE</b>	<b>BMI</b>
LA	Male	31	23.5
LI	Female	24	19.1
SM	Male	23	25
SP	Female	22	19.9
MO	Female	25	24.6
AP	Female	25	21.1
MM	Female	27	21.6
AB	Female	25	21.5
AC	Female	24	21.2
MTP	Female	23	18.3

To conduct the measurement, the mobile node is placed on the 10 subjects to detect the diaphragm contraction. Moreover, the sternum is considered as anatomical landmarks for the electrode positioning and in fact, an electrode is placed just below the lower part of the sternum and the second electrode 7 cm distant from the first, along the left part of the body, just below the rib cage. In figure 18 is shown the placement of the electrodes.

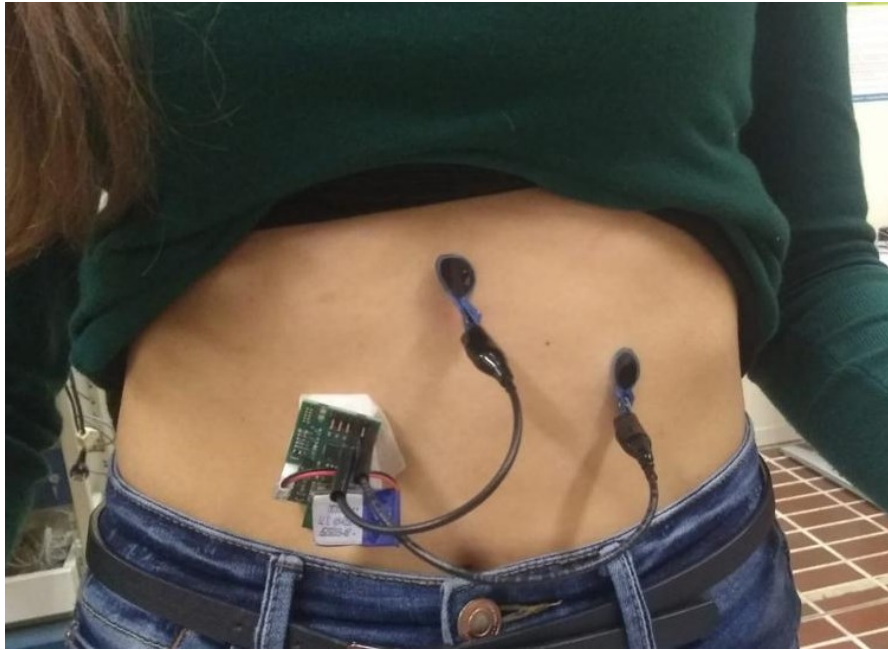


Figure 18 - Adhesive conductive electrode positioning

In a standing position, the subject was asked to perform a breaths cycle consisted in five deep breaths, each deep breath has a duration of 8 seconds (4 s inspiration and 4 s expiration) followed by five normal breaths, each normal breath has a duration of 4 seconds (2 s inspiration and 2 s expiration) repeated two times.

### 2.3 Signal Processing

Since the placement of the electrodes is quite near to the heart, the acquired diaphragmatic sEMG signal is corrupted by cardiac artefacts, for this reason, it has to be submitted to improved filtering techniques. In particular, to remove the ECG signal is firstly applied a band-pass filter with cut-off frequencies 100Hz-200Hz [9] to remove a significant amount of power. Despite this common filtering technique, the cardiac signal continues to be relevant on the diaphragmatic sEMG generated

by the diaphragm contraction, for this reason, it is applied to the filtered signal the WT, a mathematical tool suitable for the processing of non-stationary signal such as the EMG data [28] [29]. WT is used with the aim to denoise the sEMG signal, so the selected parameters to compute the denoising procedure are Coiflet of order 5<sup>th</sup> as mother wavelet, with 6 levels of decomposition and as default is applied a soft threshold. Furthermore, to attenuate the peak caused by the heart rate the denoised signal is processed by means of Principal Component Analysis (PCA) [30]. Since the signal is composed of many interrelated variables, the aim of the PCA is to reduce the dimension of the data set reducing the variability of the interrelated variables. In addition, the PCA gives as result a set of uncorrelated variables ordered in a way that the first few retain most of the variation present in all the original variables. The processing of the wavelet denoising signal by means of PCA gives the advantage to further decrease the heart rate that is still present after the filtering techniques used previously.

### 3. Results

The following figures depict the results of the acquired signal on the 10 subjects

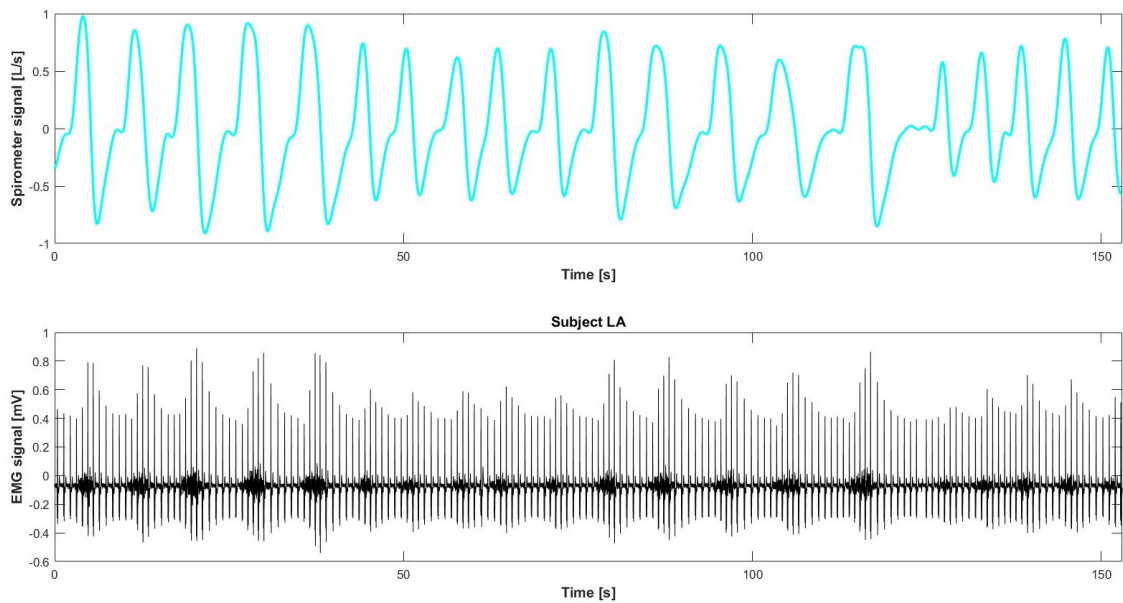


Figure 19 - Correspondence between spirometer and raw EMG signal on subject LA

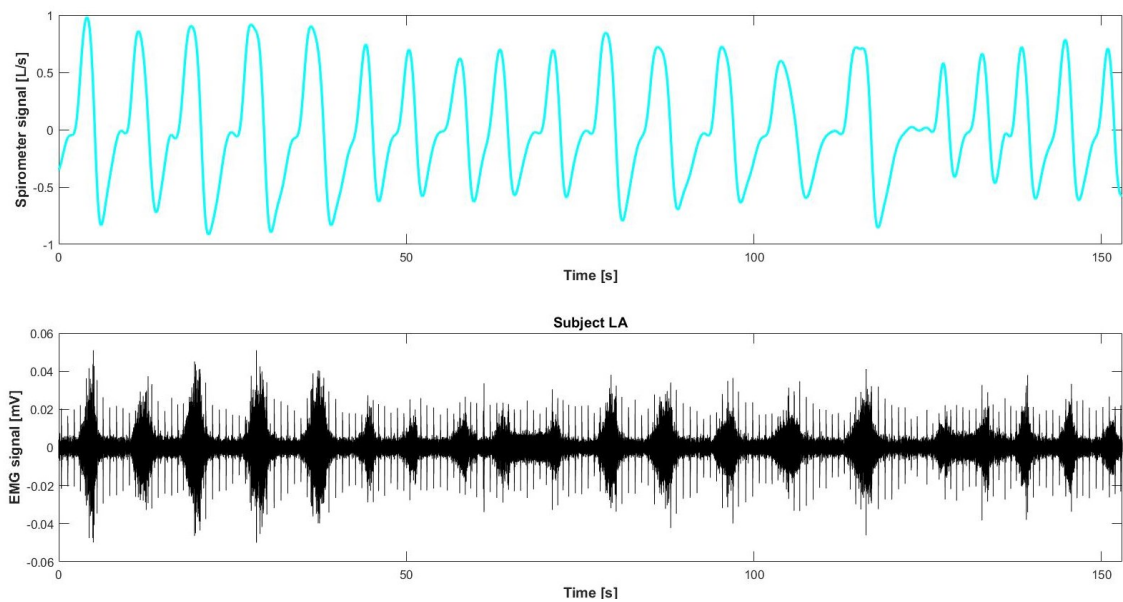


Figure 20 - Correspondence between spirometer and filtered EMG on subject LA

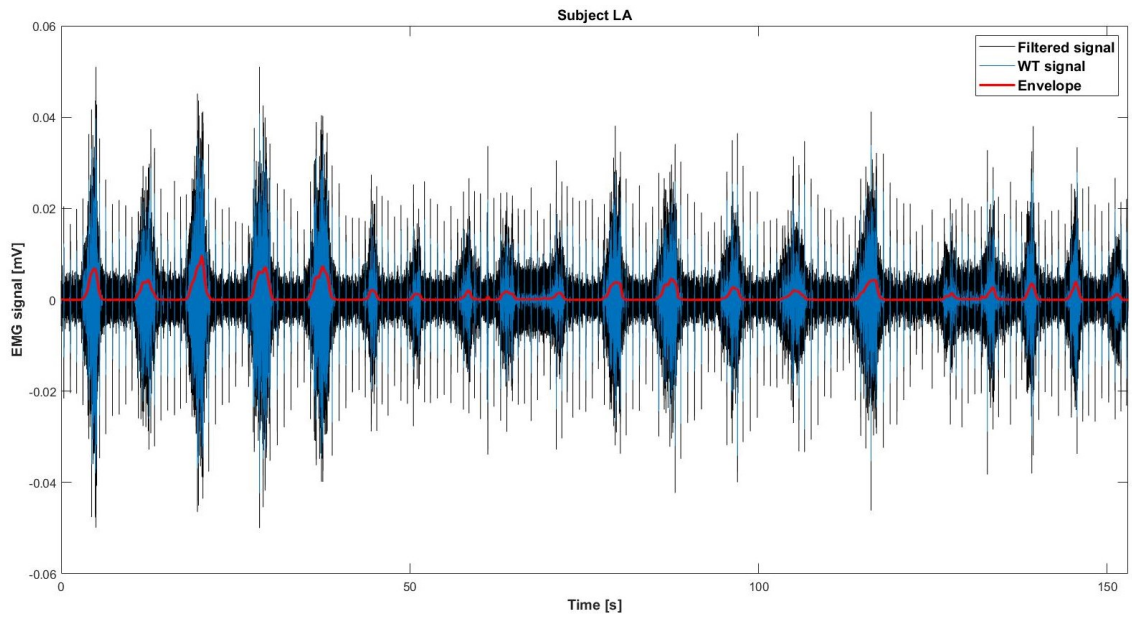


Figure 21 - Superimposition of Filtered, WT and Envelope EMG signal on subject LA

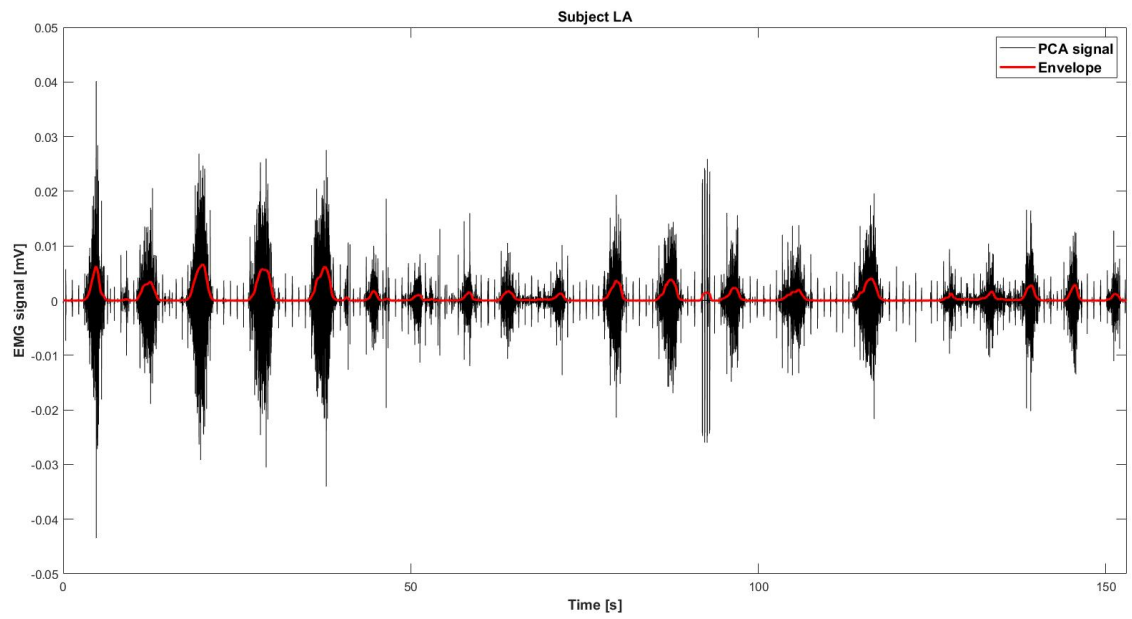


Figure 22 - Superimposition of PCA and Envelope EMG signal on subject LA

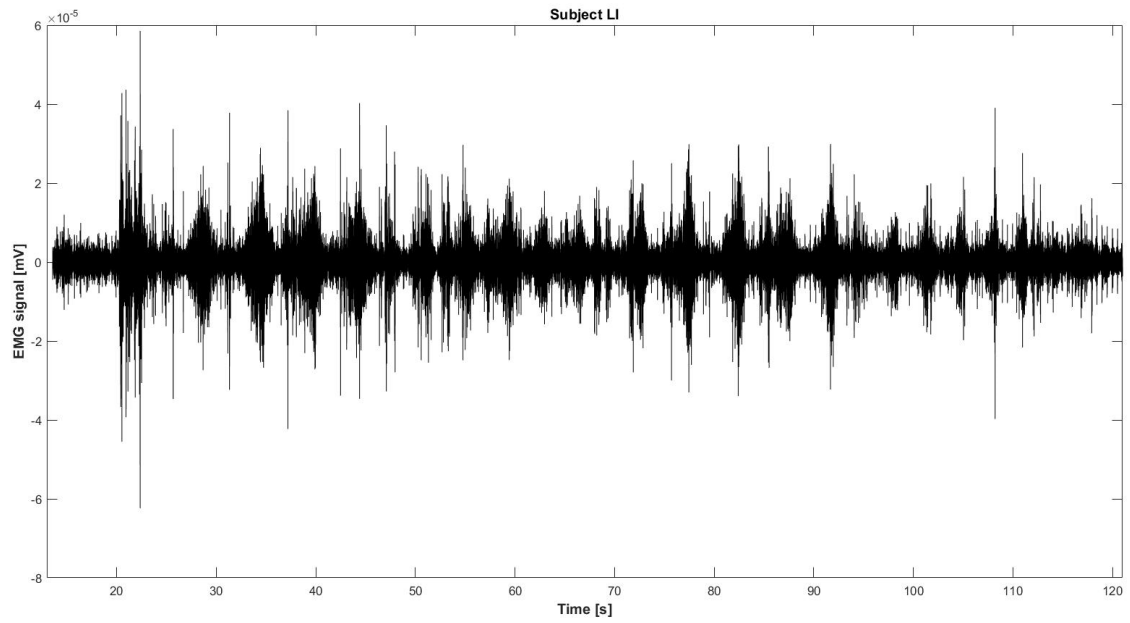


Figure 23 - Filtered EMG signal on subject LI

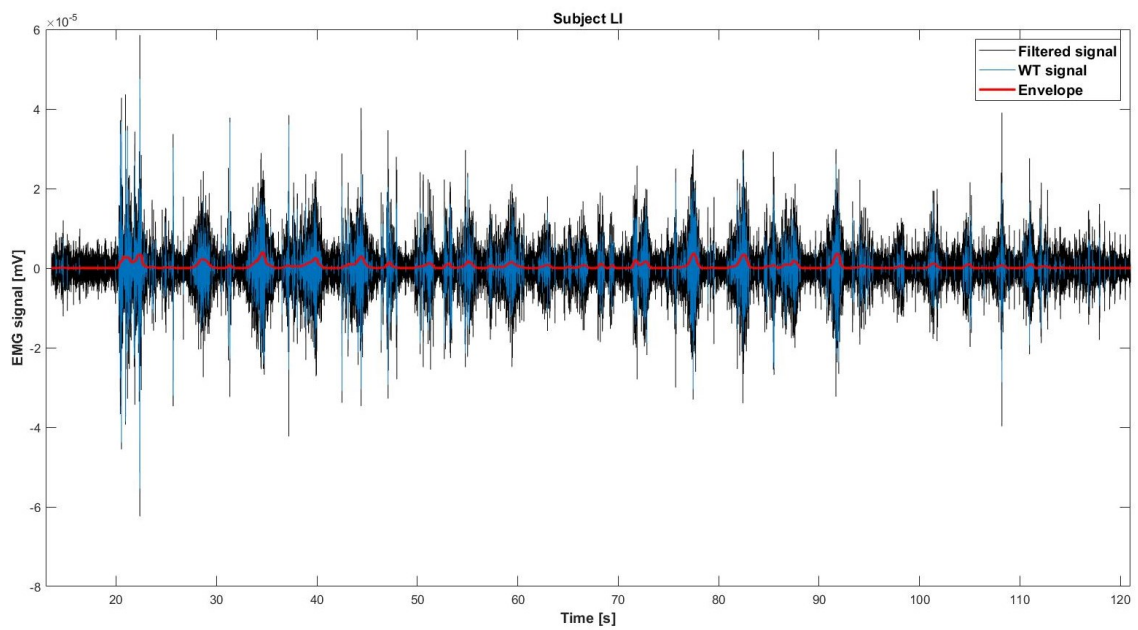


Figure 24 - Superimposition of Filtered, WT and Envelope EMG signal on subject LI

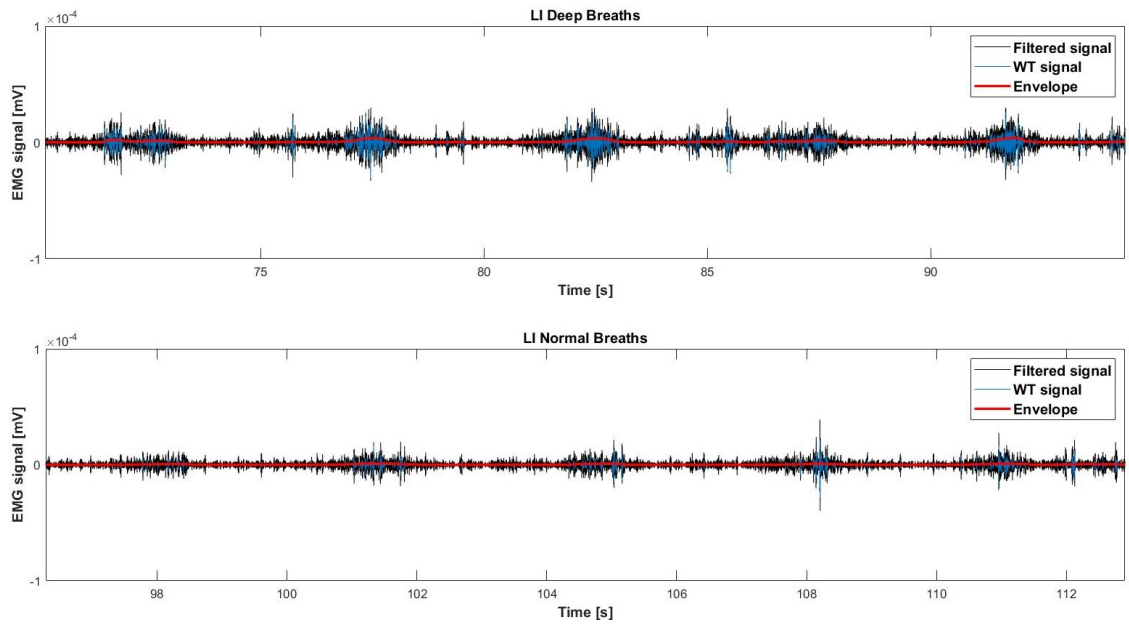


Figure 25 - Alternation of deep and normal breaths on subject LI

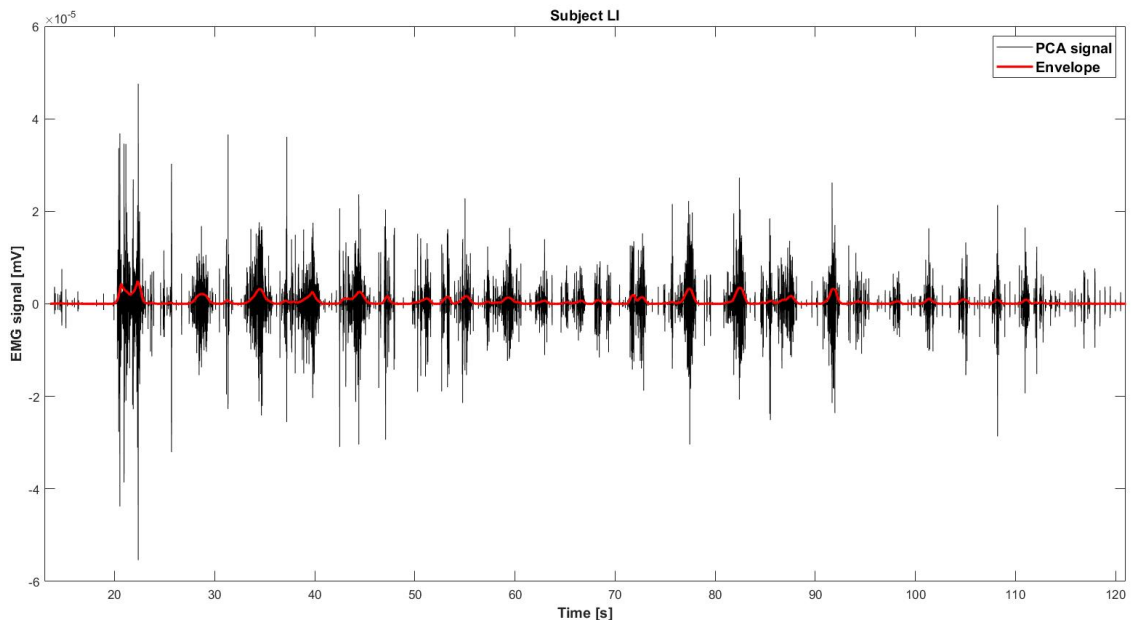


Figure 26 - Superimposition of PCA and Envelope EMG signal on subject LI

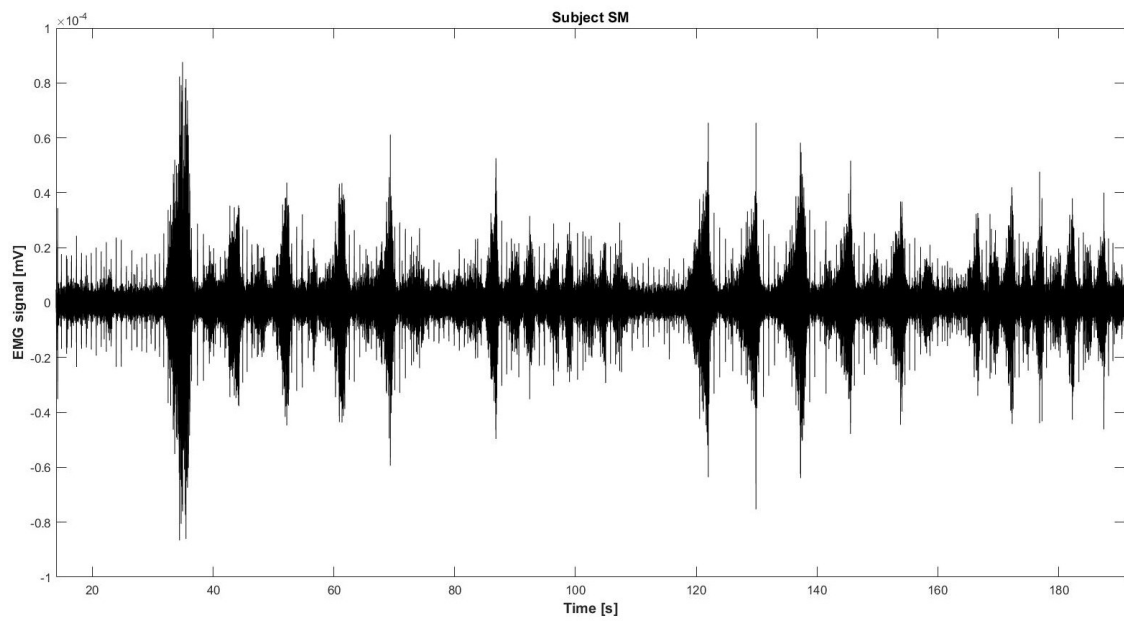


Figure 27 - Filtered EMG signal on subject SM

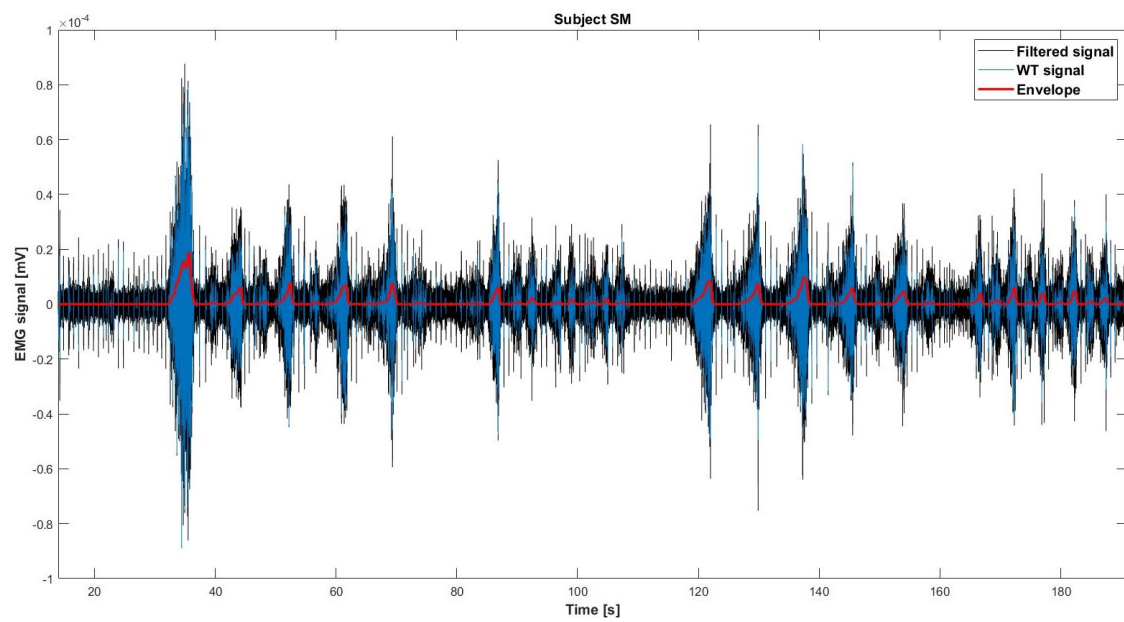


Figure 28 - Superimposition of Filtered, WT and Envelope EMG signal on subject SM

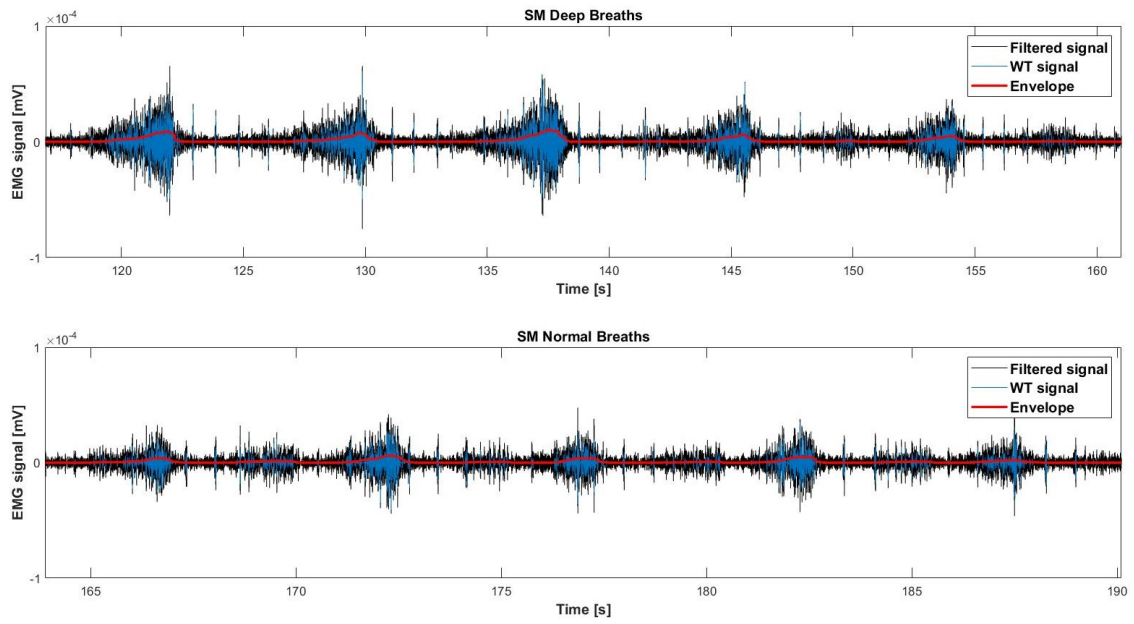


Figure 29 - Alternation of deep and normal breaths on subject SM

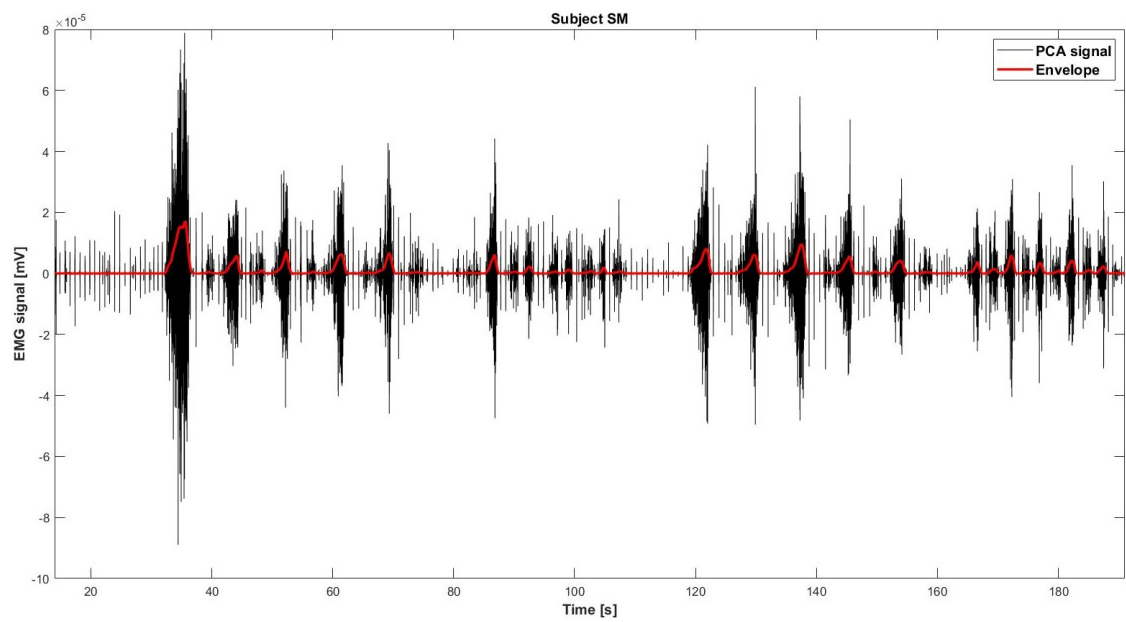


Figure 30 - Superimposition of PCA and Envelope EMG signal on subject SM

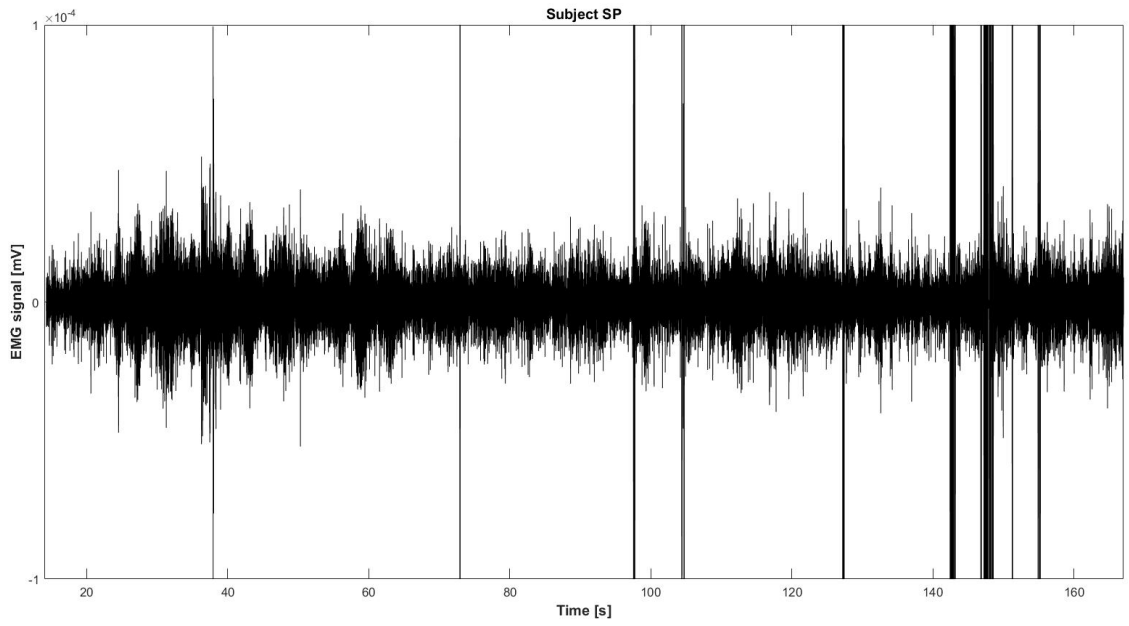


Figure 31 - Filtered EMG signal on subject SP

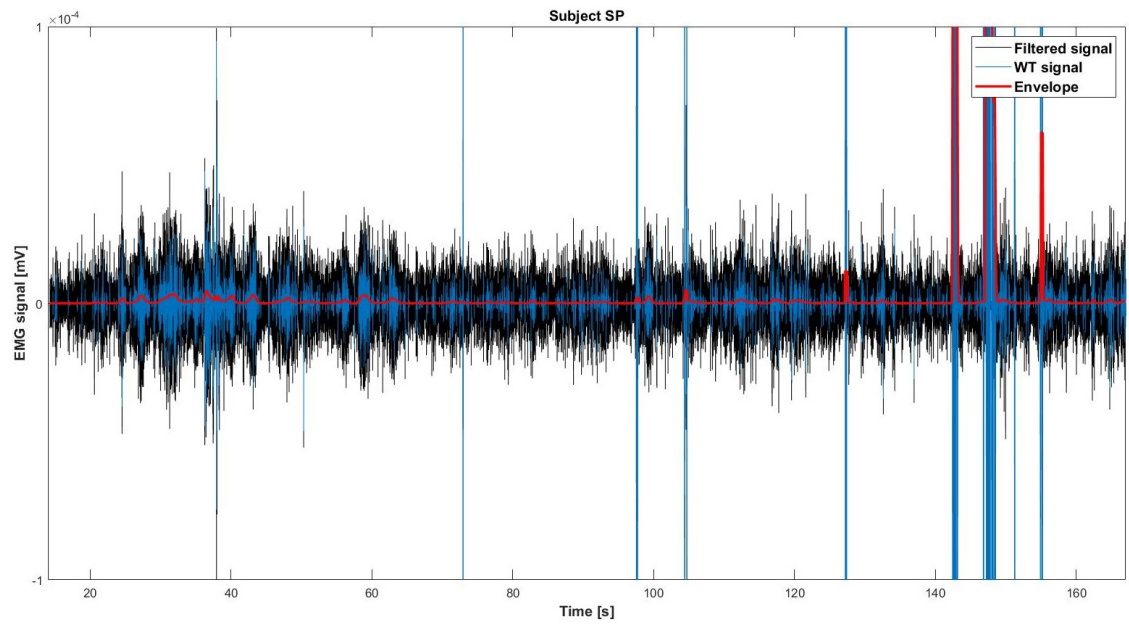


Figure 32 - Superimposition of Filtered, WT and Envelope EMG signal on subject SP

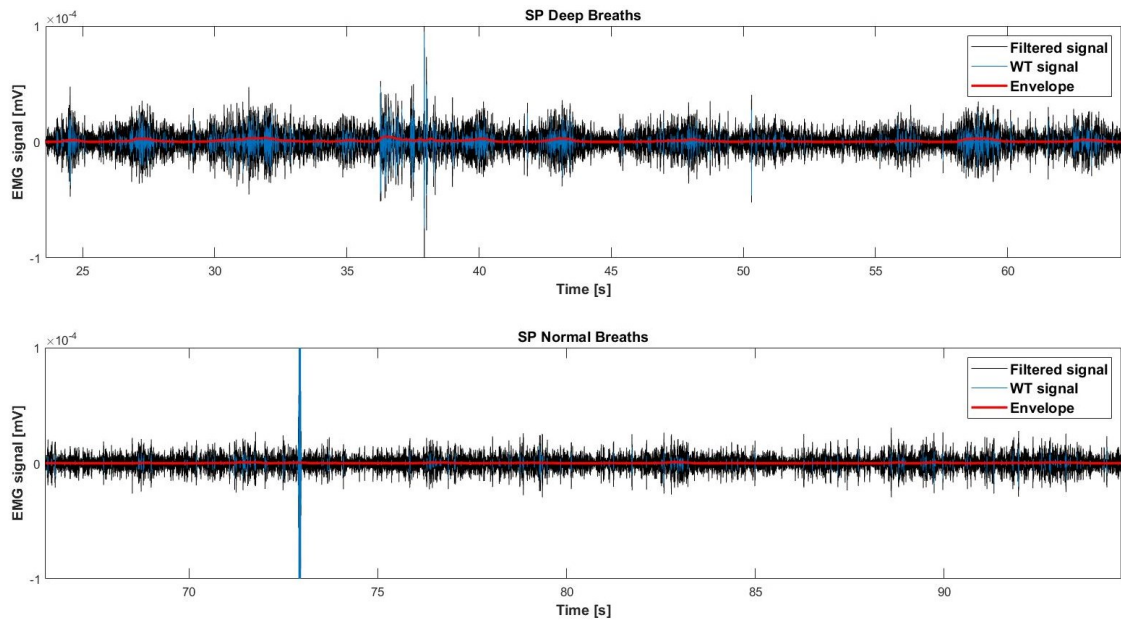


Figure 33 - Alternation of deep and normal breaths on subject SP

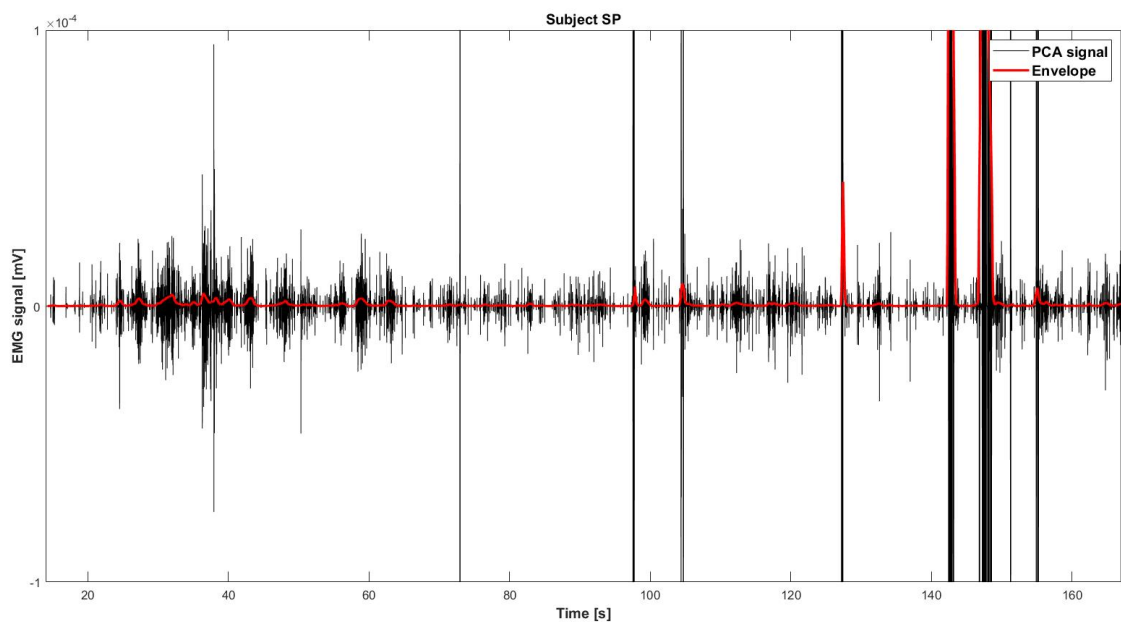


Figure 34 - Superimposition of PCA and Envelope EMG signal on subject SP

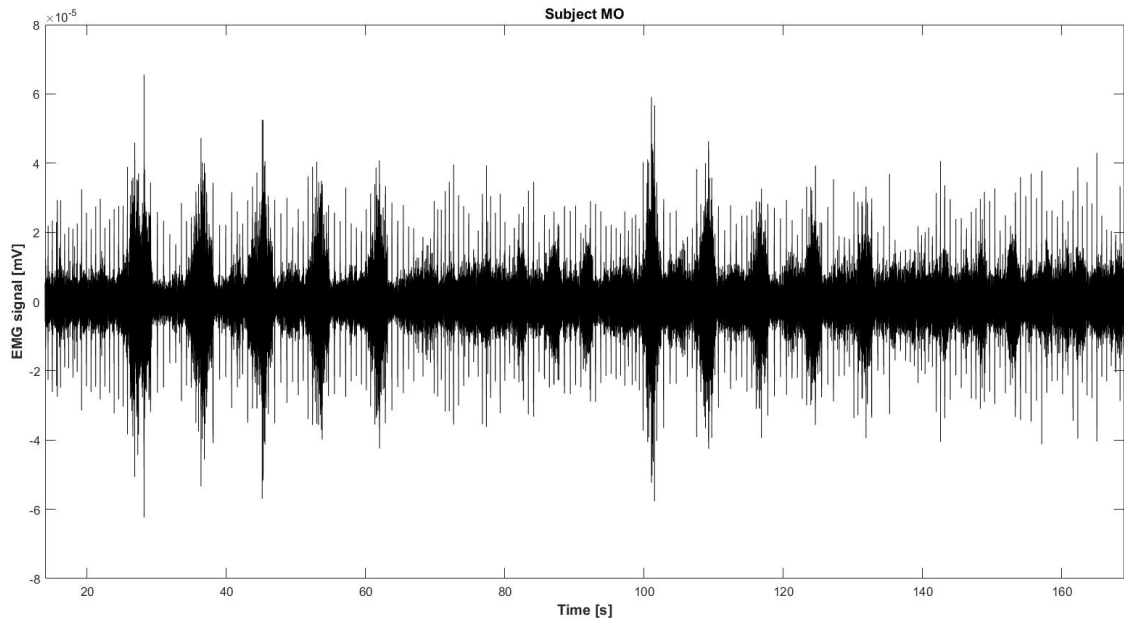


Figure 35 - Filtered EMG signal on subject MO

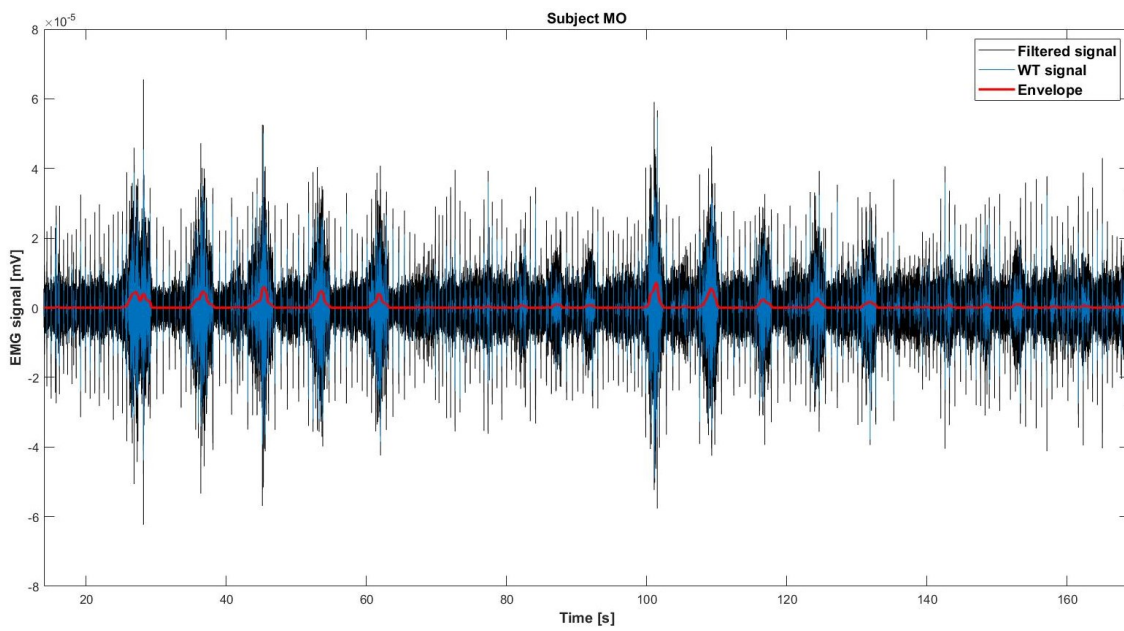


Figure 36 - Superimposition of Filtered, WT and Envelope EMG signal on subject MO

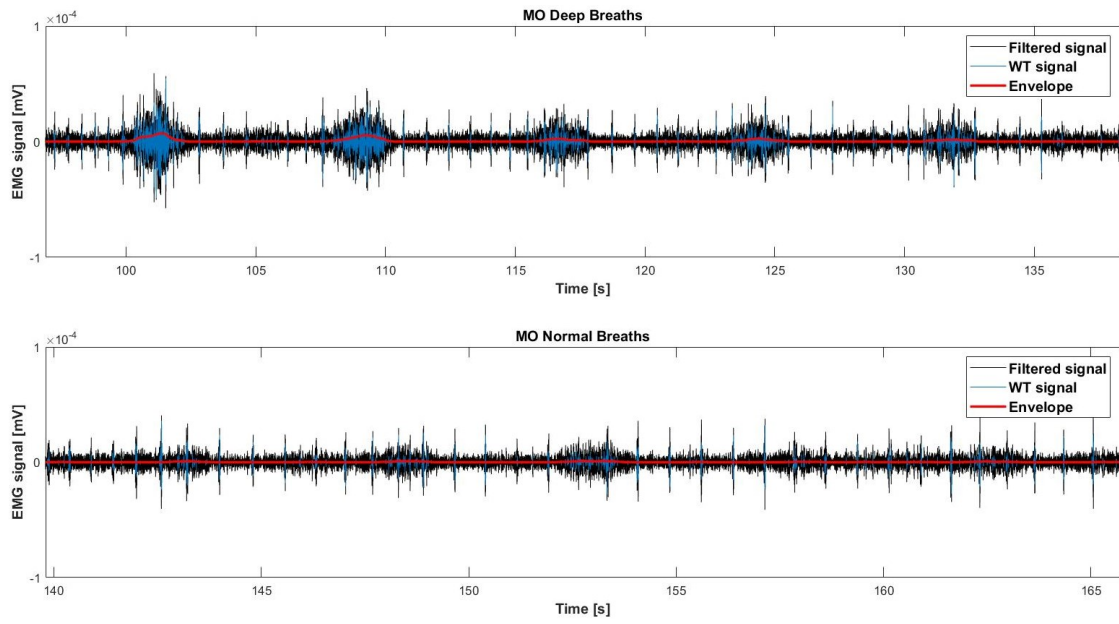


Figure 37 - Alternation of deep and normal breaths on subject MO

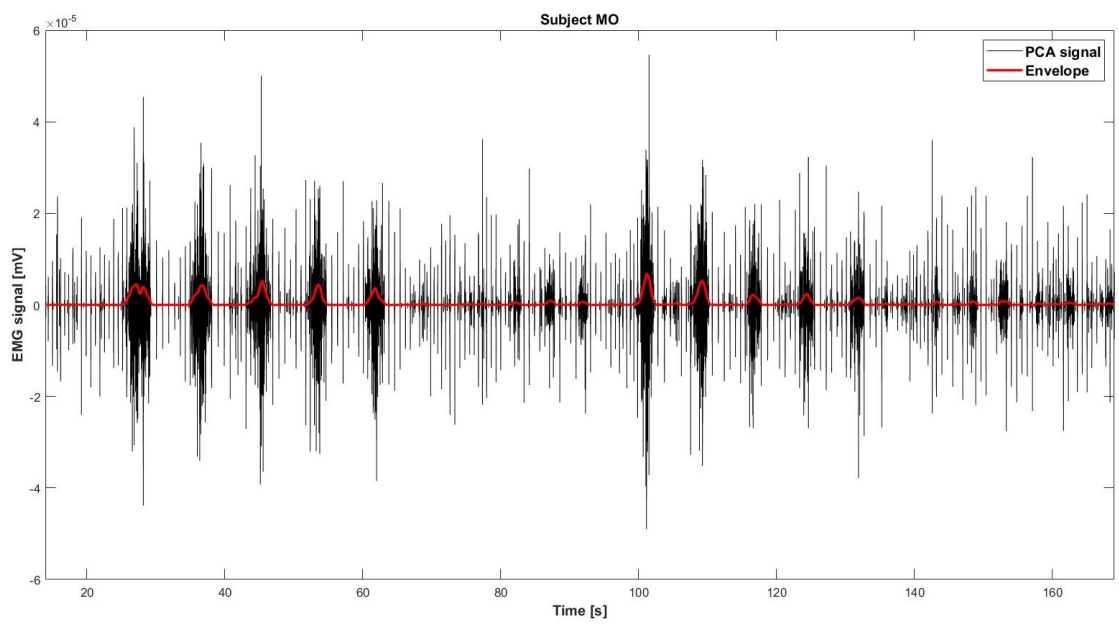


Figure 38 - Superimposition of PCA and Envelope EMG signal on subject MO

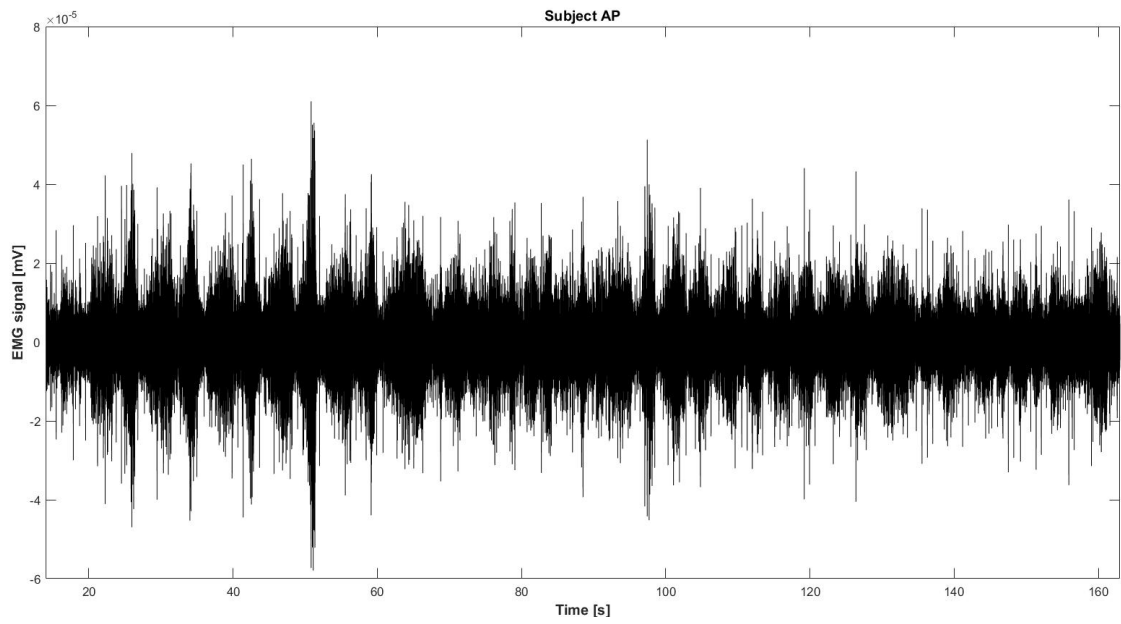


Figure 39 - Filtered EMG signal on subject AP

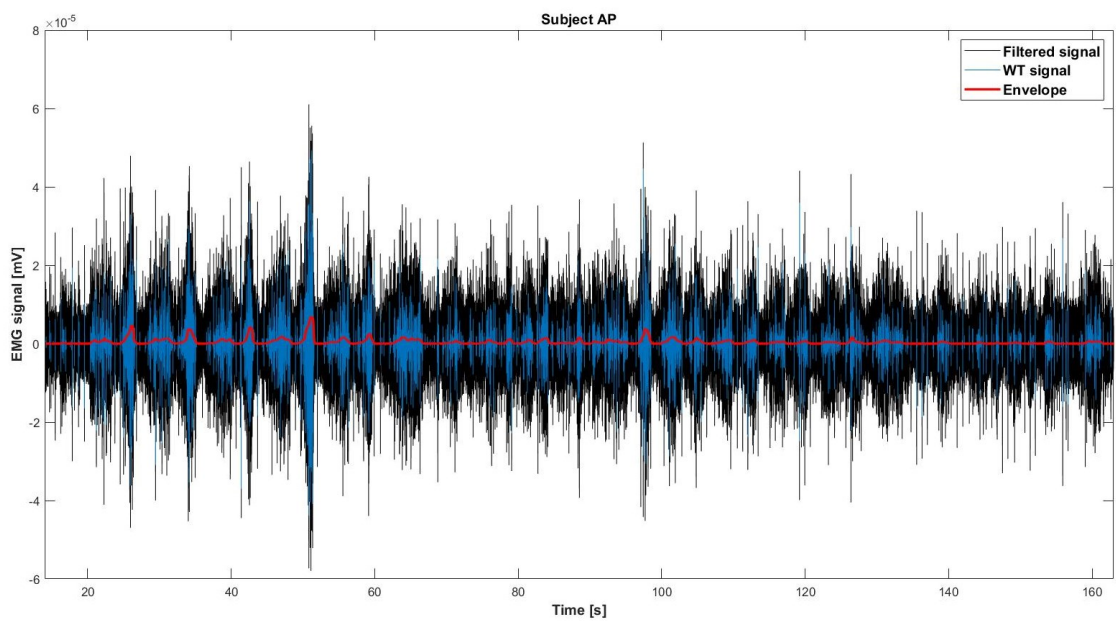


Figure 40 - Superimposition of Filtered, WT and Envelope EMG signal on subject AP

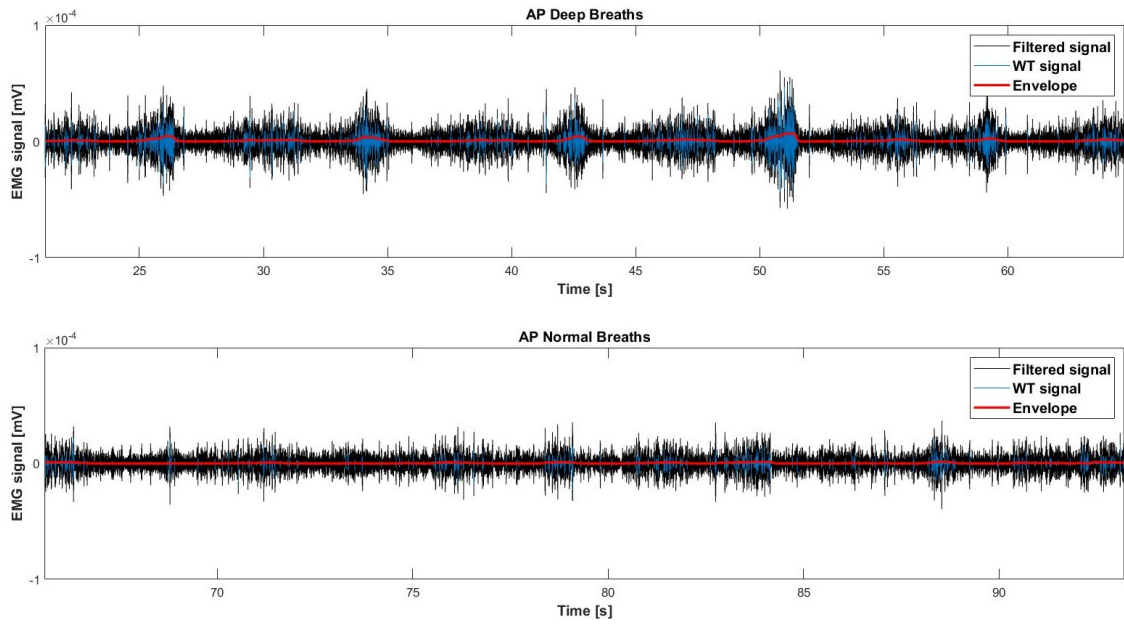


Figure 41 - Alternation of deep and normal breaths on subject AP

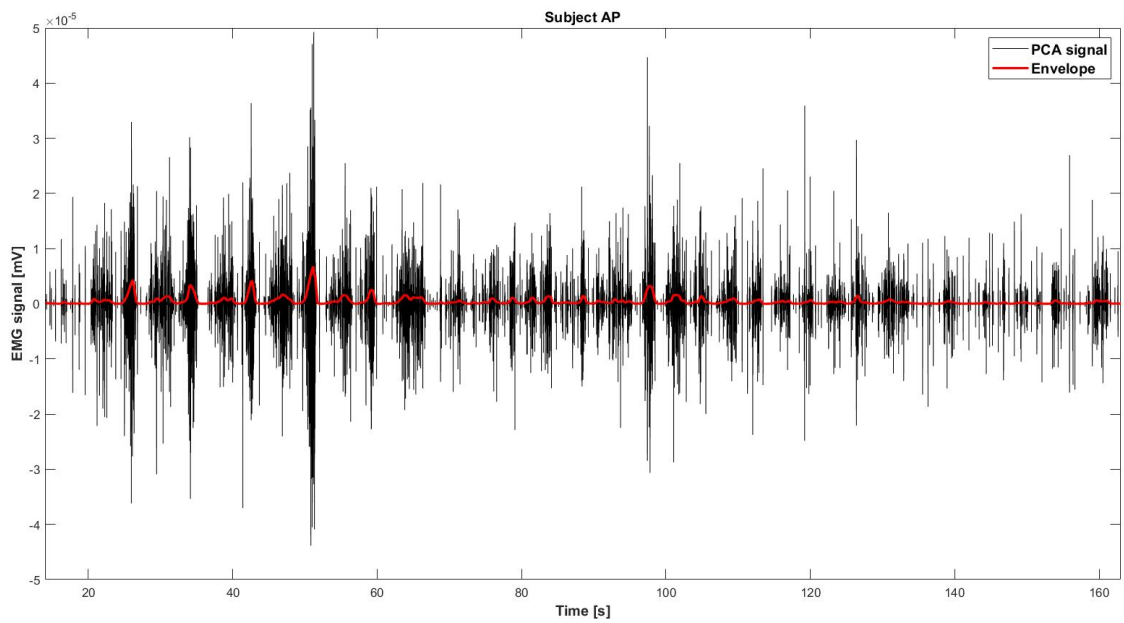


Figure 42 - Superimposition of PCA and Envelope EMG signal on subject AP

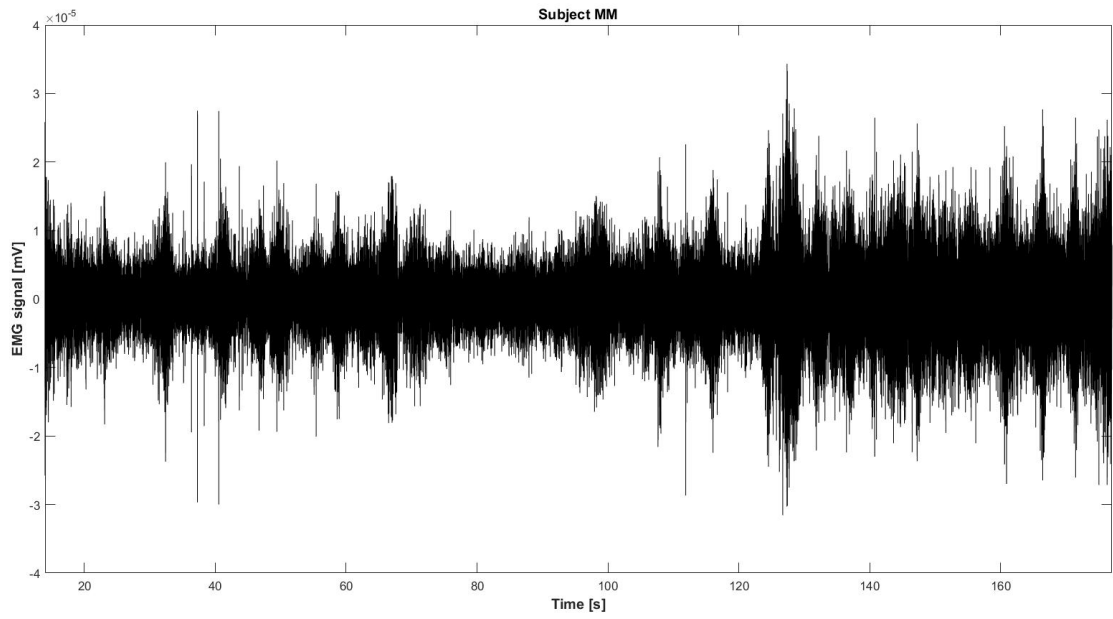


Figure 43 - Filtered EMG signal on subject MM

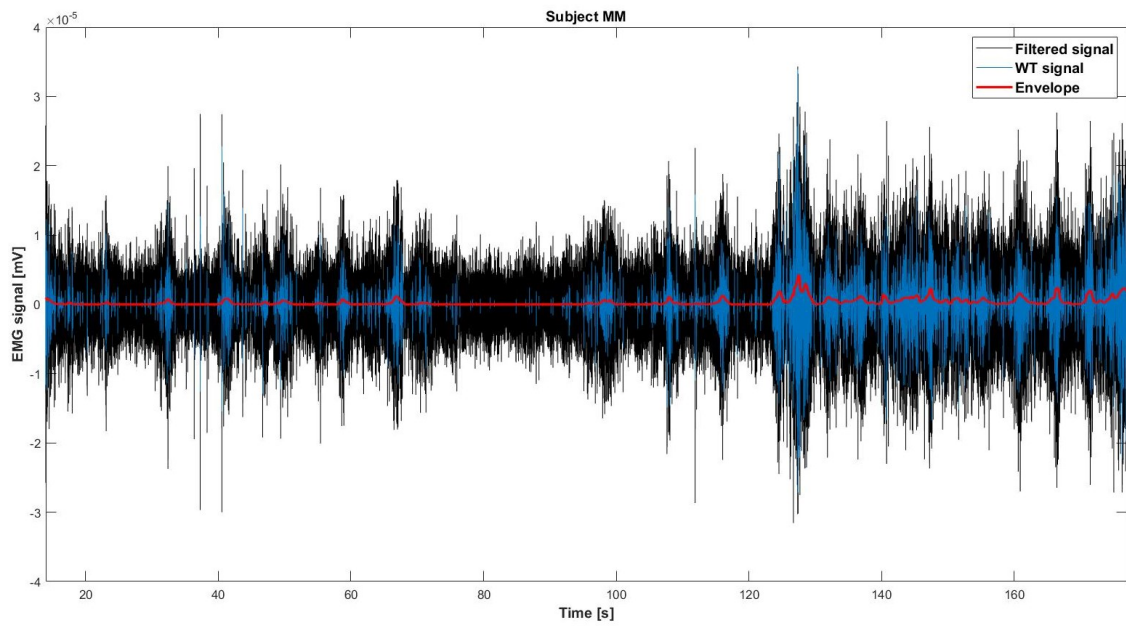


Figure 44 - Superimposition of Filtered, WT and Envelope EMG signal on subject MM

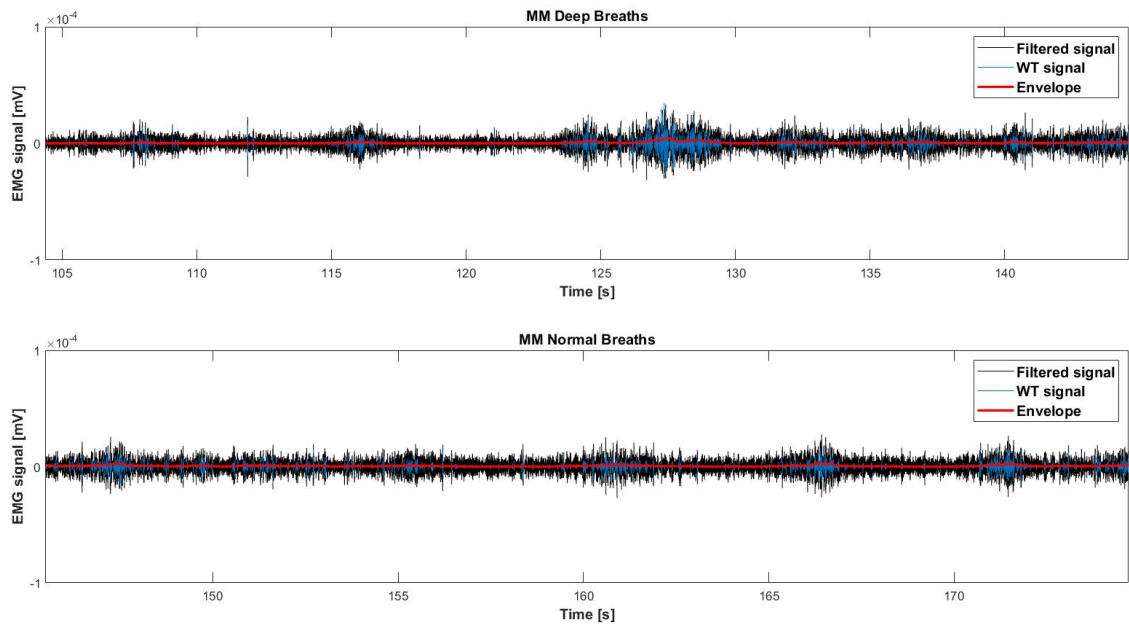


Figure 45 - Alternation of deep and normal breaths on subject MM

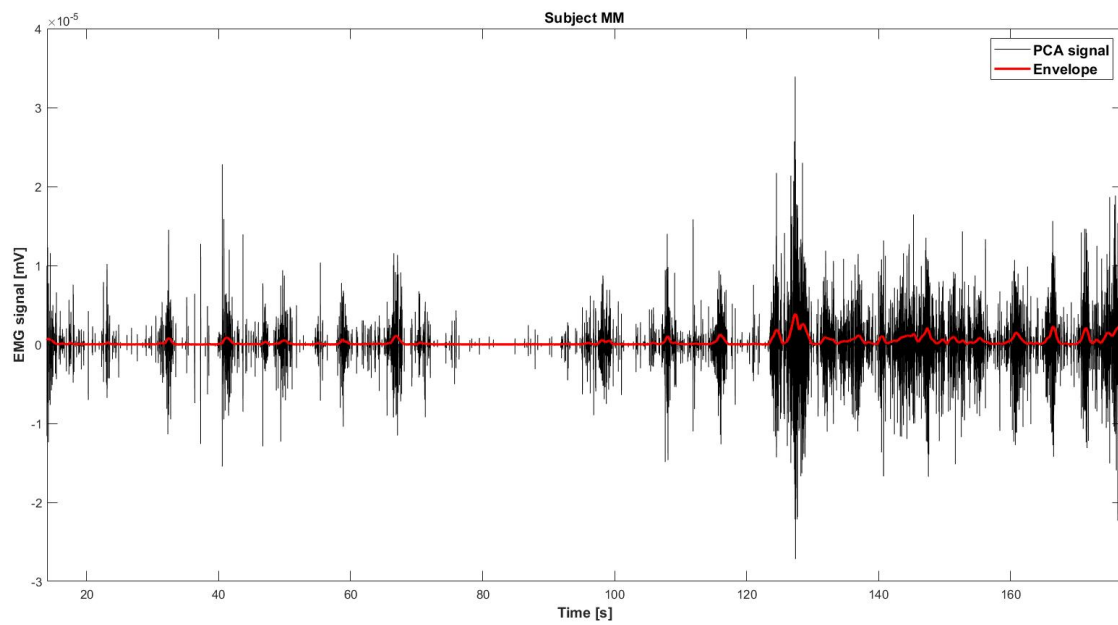


Figure 46 - Superimposition of PCA and Envelope EMG signal on subject MM

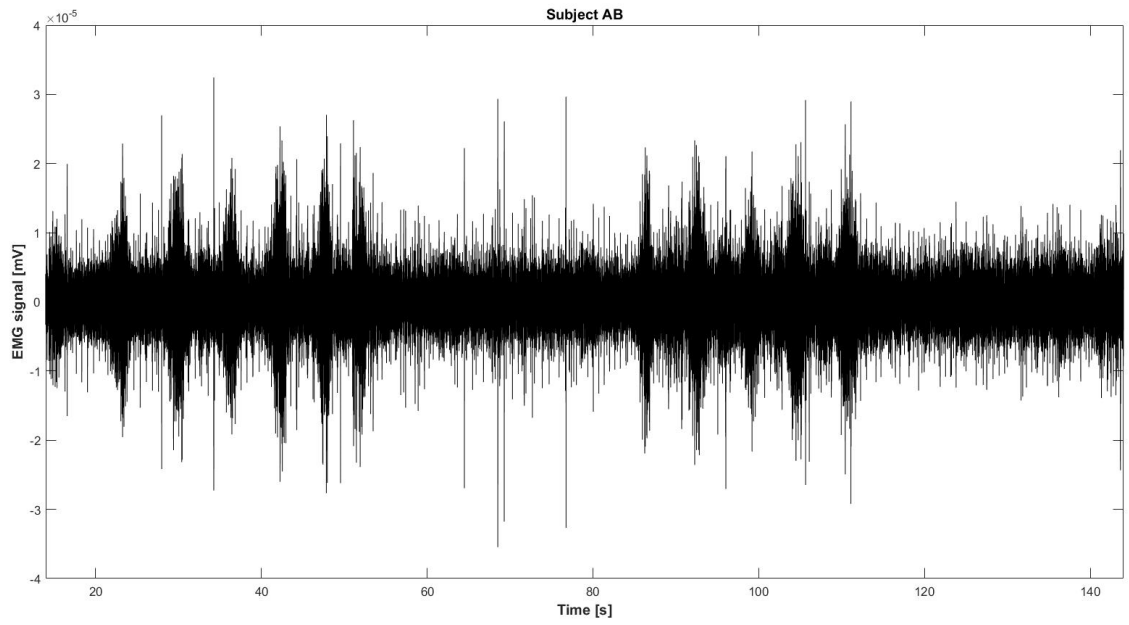


Figure 47 - Filtered EMG signal on subject AB

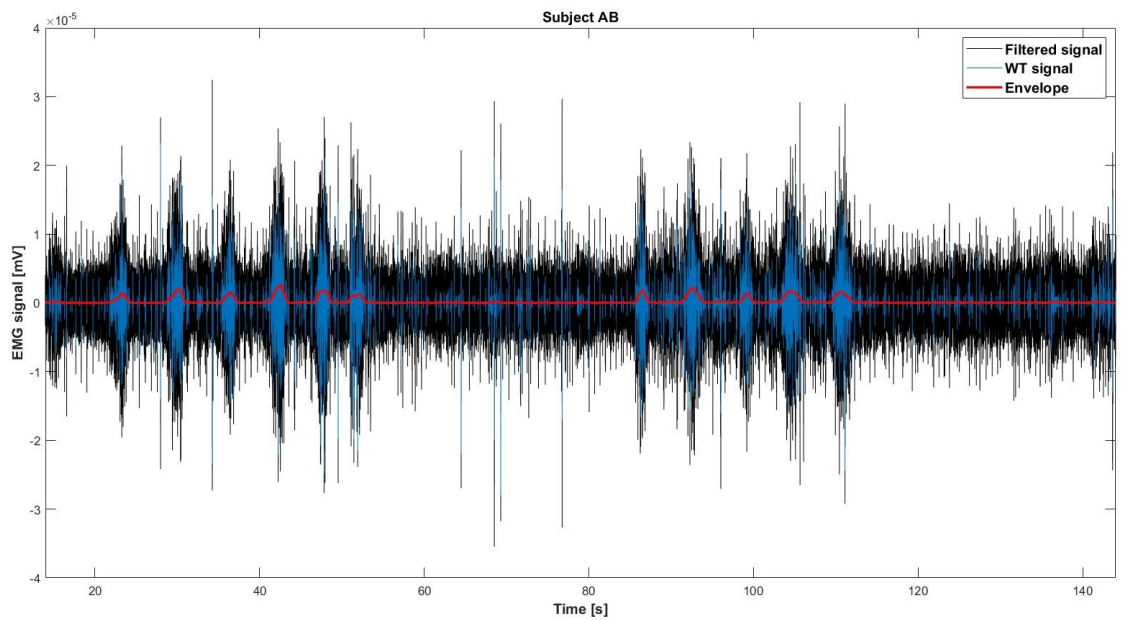


Figure 48 - Superimposition of Filtered, WT and Envelope EMG signal on subject AB

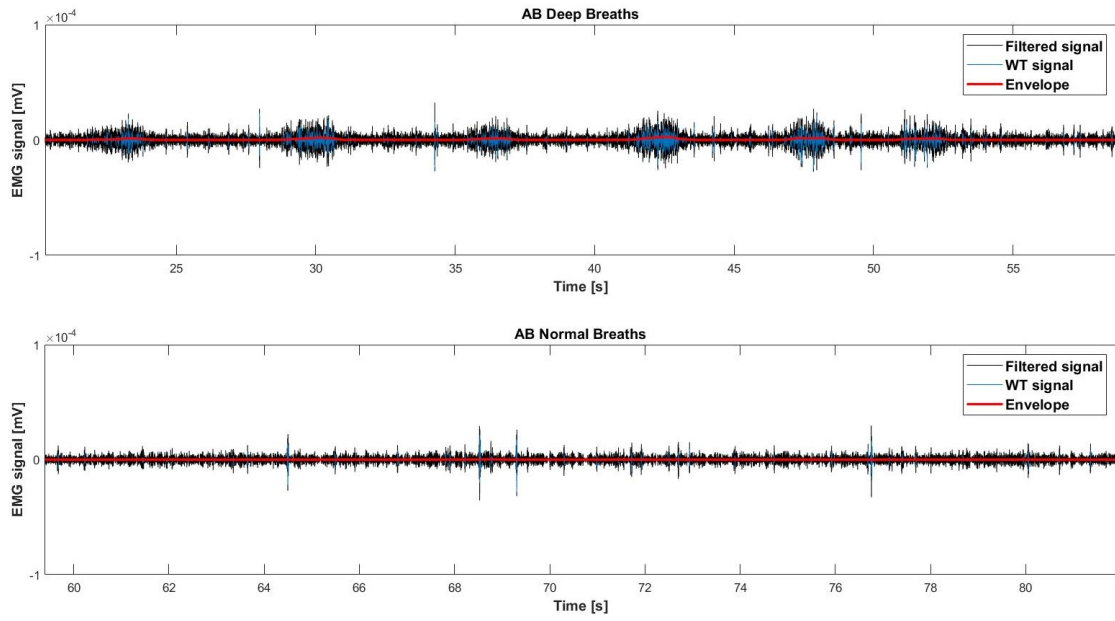


Figure 49 - Alternation of deep and normal breaths on subject AB

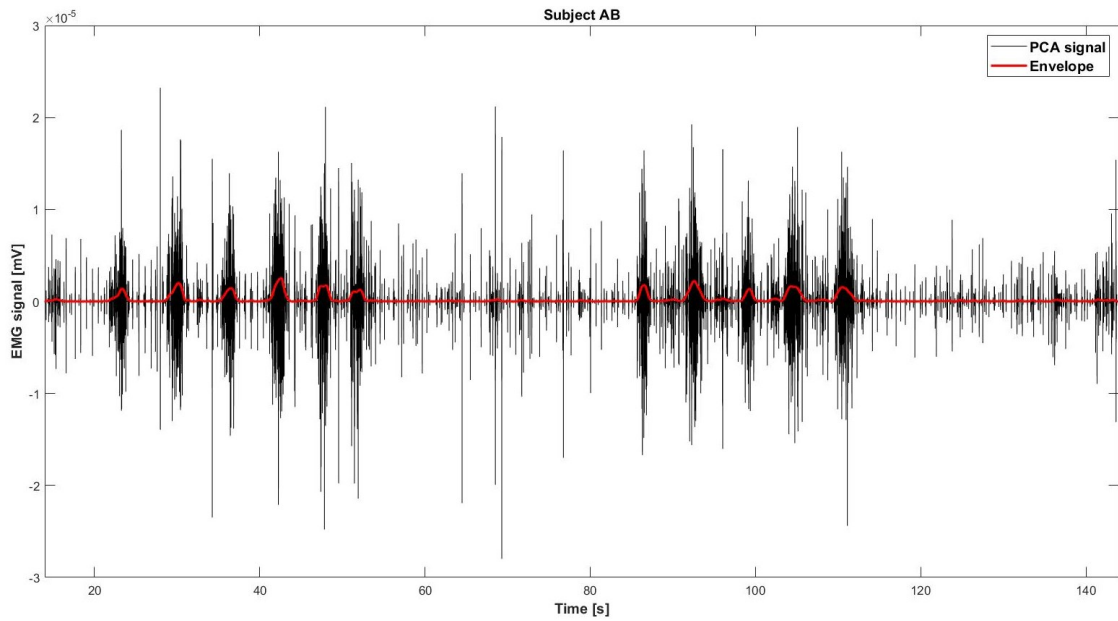


Figure 50 - Superimposition of PCA and Envelope EMG signal on subject AB

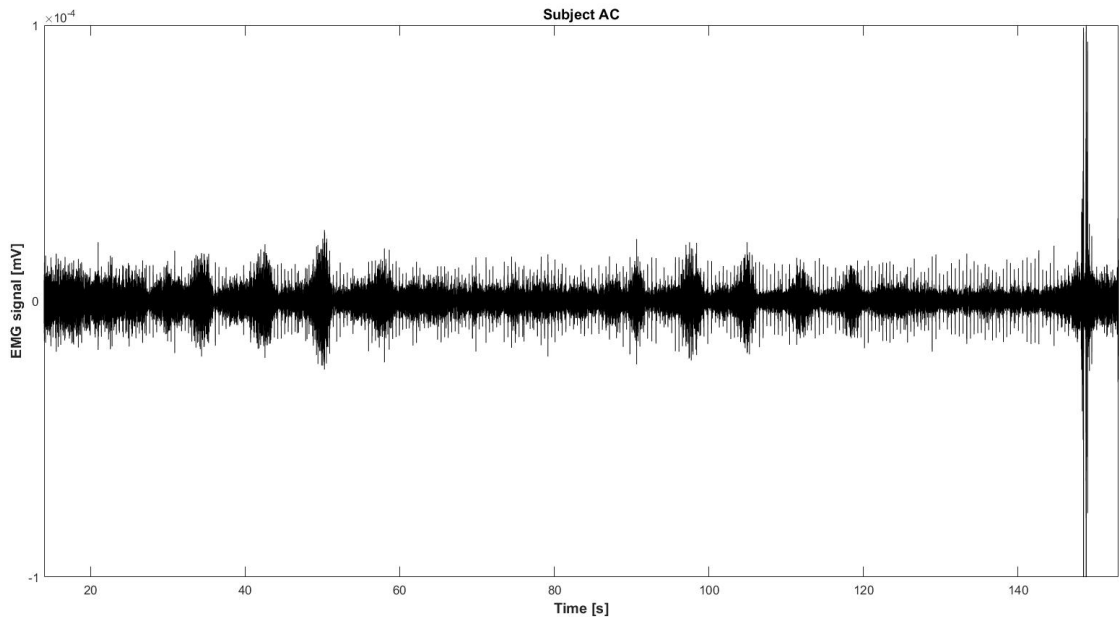


Figure 51 - Filtered EMG signal on subject AC

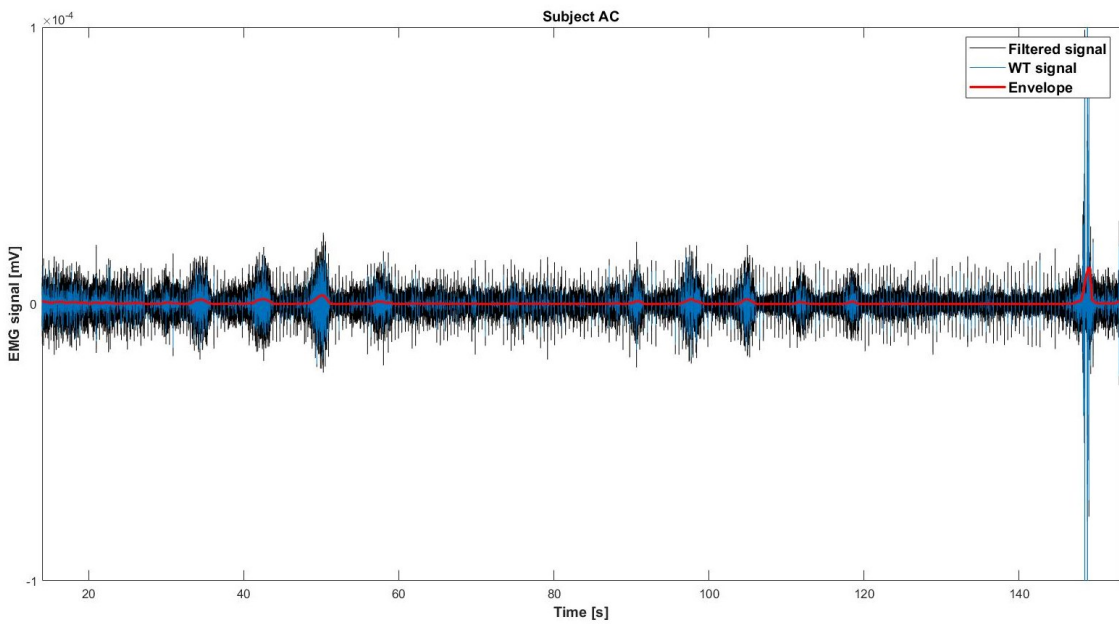


Figure 52 - Superimposition of Filtered, WT and Envelope EMG signal on subject AC

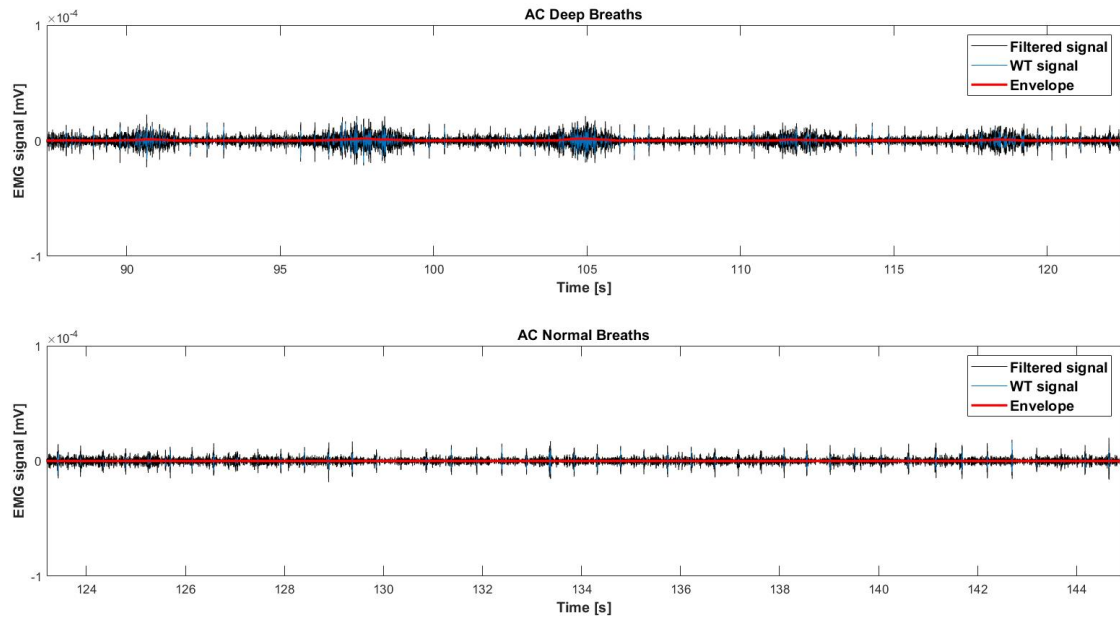


Figure 53 - Alternation of deep and normal breaths on subject AC

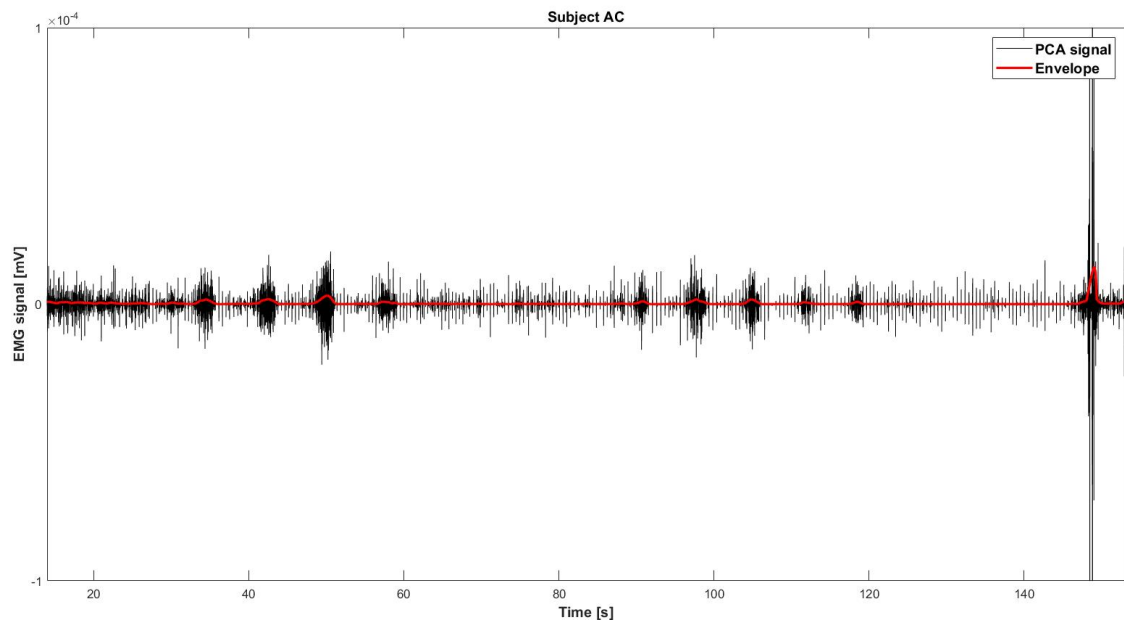


Figure 54 - Superimposition of PCA and Envelope EMG signal on subject AC

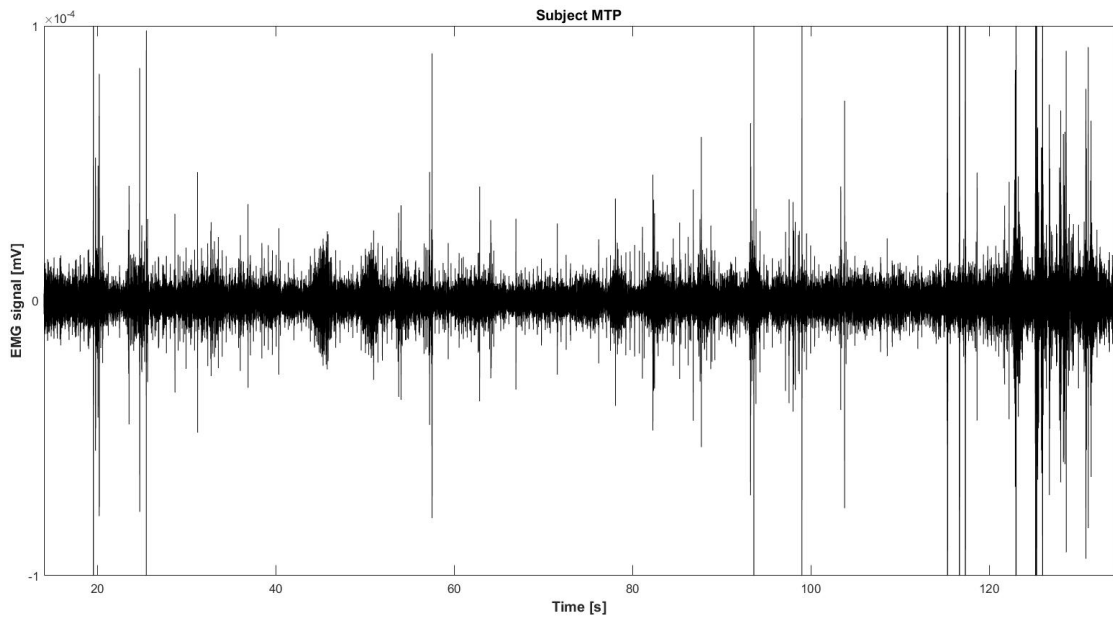


Figure 55 - Filtered EMG signal on subject MTP

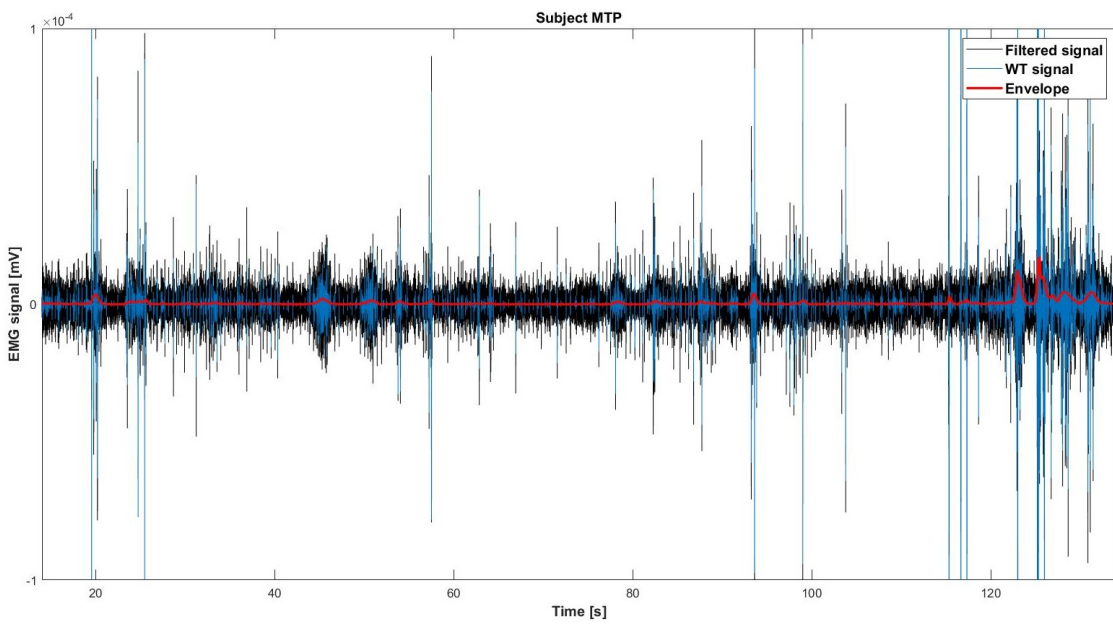


Figure 56 - Superimposition of Filtered, WT and Envelope EMG signal on subject MTP

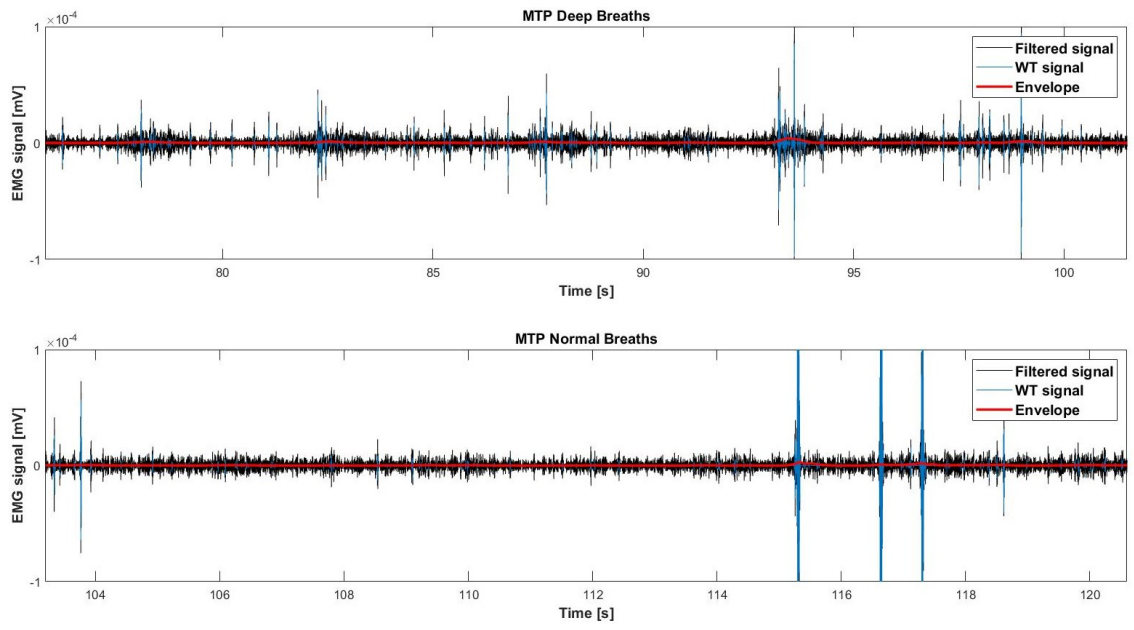


Figure 57 - Alternation of deep and normal breaths on subject MTP

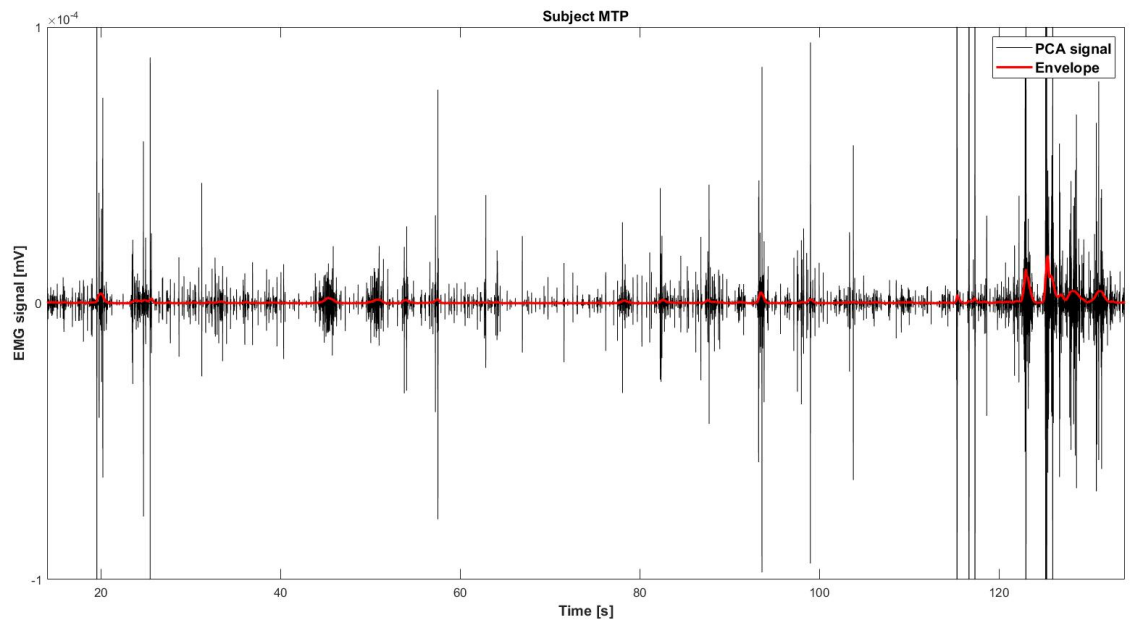


Figure 58 - Superimposition of PCA and Envelope EMG signal on subject MTP

The following table resumes the envelope amplitude and the SNR in deep and normal breaths computed in all the voluntary subjects.

Table 4 – Envelope amplitude and SNR in deep and normal breaths.

ID	Deep breath envelope	Normal breath envelope	Deep breath SNR	Normal breath SNR
LA	0.007 mV	0.003 mV	56.1	25.5
LI	$3,4 \cdot 10^{-6}$ mV	$1.6 \cdot 10^{-6}$ mV	22.7	18.3
SM	$9.4 \cdot 10^{-6}$ mV	$6.0 \cdot 10^{-6}$ mV	31.2	18.5
SP	$2.8 \cdot 10^{-6}$ mV	$9.9 \cdot 10^{-7}$ mV	86.9	83.7
MO	$6.7 \cdot 10^{-6}$ mV	$9.1 \cdot 10^{-7}$ mV	14.8	8.9
AP	$6.8 \cdot 10^{-6}$ mV	$1.5 \cdot 10^{-6}$ mV	36.4	12.4
MM	$8.7 \cdot 10^{-7}$ mV	$2.0 \cdot 10^{-7}$ mV	25.3	11.9
AB	$2.5 \cdot 10^{-6}$ mV	$2.8 \cdot 10^{-7}$ mV	12.3	0.7
AC	$3.2 \cdot 10^{-6}$ mV	$2.8 \cdot 10^{-7}$ mV	17.2	2.8
MTP	$2.03 \cdot 10^{-6}$ mV	$4.0 \cdot 10^{-7}$ mV	22.2	20.3

## 4. Discussion

From the evaluation of the results, it is clear that the diaphragmatic activity is corrupted by a lot of noise that comes from the heart. Despite the SENIAM protocol [7] suggests for sEMG signal cut-off frequencies of 20 Hz -450 Hz, in this situation they weren't suitable not only because of the discordance with the sampling theorem, being the sampling frequency equal to 800 Hz, moreover, such filtration removes a high content of information coming from the interested muscle. For this reason, it has been preferred a band-pass filter with cut-off frequencies at 100 Hz -200 Hz [9]. Subsequently, the filtered signal has been submitted to WT and PCA denoising techniques but the signal is still corrupted by the cardiac artefacts [28] [29] [30]. In order to identify the contraction of the diaphragm provoked by deep and normal breaths, it has computed the envelope of the signal with a low pass filter of 5 Hz as a cut-off frequency.

Another important consideration concerning the cardiac artefacts that should be taken under consideration is related to the electrodes positioning. The systematic review of Masselli et al. [13] considers that different researches place the electrodes in different positions to try to avoid the cardiac artefacts. They take into account many positions ranging from the 5<sup>th</sup> and 10<sup>th</sup> intercostal space to the 7<sup>th</sup> and 8<sup>th</sup> intercostal space taking the midclavicular axillary line as anatomical landmark and the sternum as place in which put the reference electrodes.

Starting from the consideration obtained from Masselli et al. [13], in this study is decided to vary the inter-electrodes distance taking as anatomical landmark the sternum. In particular, placing the electrode on the sternum, the position of the second electrode is decided testing many distances, in particular, the tested distances are 10 cm, 9 cm, 8 cm, and 7 cm. The best inter-electrode distance that reduces the presence of cardiac artefacts is obtained with 7 cm. The reason could be justified by the fact that placing the two electrodes near between themselves and directed parallel to the muscular fibers, the signal coming from the muscle fibers has a higher intensity than the signal coming from the source of the noise.

However, despite this electrode positioning that reduces the cardiac artefact, the signal is still corrupted by noise.

In addition, an important parameter that has to be considered is the ability to discerning the diaphragmatic respiration from the pulmonary respiration. In fact, the results provide proof that not all of the involved voluntary participants completely use the diaphragm muscle during the respiratory cycle. Obviously, the values of the envelope computed in the deep and normal breaths, resumed in table 4, highlight the fact that in all of the subjects, the deep breaths are more evident respect to the normal breaths, because they involve a muscle activation higher respect to the normal breaths. This fact is confirmed even by the higher SNR that characterize the deep breaths respect to the normal breaths in all the voluntary subjects. However, the signal obtained from some participants (SP and MTP), is even corrupted by motion artefact, evident as spikes in the sEMG tracing that makes difficult the identification of normal breaths. A solution to this motion problem could be dealt with changing the standing position with lying down position in which the subject is limited in the movement facilitating the diaphragmatic contraction and relaxation.

For what concerns the materials of the adhesive conductive electrodes, it is necessary to do some considerations. The Bare Conductive electric paint is able to perfectly conduct the biological signal thanks to the presence of conductive carbon between its ingredients. The hydrogel adhesive patch, with its flexibility and elasticity, can be adapted perfectly to the patient skin, but some recording sessions have been repeated because of their detachment, in particular on a male subject, but this problem can be solved by shaving and pre-treating the interested region to favourite a better adhesion. However, the advantage of these electrodes is that they can be produced in customized dimensions according to the type of muscle and activity that have to be recorded avoiding the problem of the cross-talks induced by a larger electrode diameter.

In addition, it is important to take into account the information derived by the Body Mass Index (BMI), in fact, the adipose tissue can cover the diaphragm information content even if in this study this problem is not present because all the analysed subjects are control subject with a normal BMI.

However, the possibility to conduct these measurements about the diaphragm contraction by means of a wireless device allows to understand the importance of the development of a wireless EMG device that not only can be used for clinical recording and sportive activities, but also in the continuous monitoring of patient with respiratory disease that requires assisted ventilation avoiding the disturbance introduced by long patient wires.

Furthermore, future studies can be employed on the application of this method in neonatal intensive care unit (NICU) patients, in which the pre-terms baby is often under assisted ventilation. In fact, the employment of this technique could be useful not only to discern the neonatal respiratory activity from the ventilator, but also to obtain a clearer sEMG than the ones obtained from the adults due to the fact that the neonatal respiratory muscles are more developed that the other that can introduce source of noise and moreover, they are characterized by a lower amount of adipose tissue respect to the adult.

#### 4.1 Limitation of the study

A limitation of this study could be represented by a lack of standardization in the deposition of the electric paint. In fact, since the development of the adhesive conductive electrode is a hand-made process, the amount of electric paint that is deposit on the adhesive gel is not fixed. To improve this technique could be suitable the employment of other materials, such as filament of thermoplastic polyurethane (TPU) mixed with conductive particles that will be directly deposited on a TPU base by the 3D print, making the developing process more precise and reproducible [31].

The electrode positioning presents some issues because even if their adopted position, selected taking into account the sternum as anatomical landmarks and 7 cm as inter-electrode distance, is the best for the sEMG recording, this does not mean that for all the participants the selected position is optimal for the recording of the diaphragm contraction because it is influenced by the anthropometric characteristics of the subjects.

In addition, the proposed filtering techniques are able to attenuate the signal coming from the heart, but as is possible to see from the pictures in the results session, they are still corrupted by noise, for this reason, an approach based on the subtraction of the ECG signal from the EMG tracing maybe could provide a clearer EMG signal.

## 5. Conclusion

The coupling of the adhesive conductive electrodes realized with conductive paint deposits on the adhesive gel patch and the wireless device developed by the Electronic group of the Department of Information Engineering of Università Politecnica delle Marche is able to detect the movement produced by the diaphragmatic contraction on sEMG tracing. The possibility to choose the correct electrode dimension offered by a customized developing process allows the recording of muscle activities produced by smaller muscle and to avoid the contamination of the other muscle that introduces noise source.

The usage of a wireless EMG device makes possible the recording of the signal avoiding the discomfort introduced by the presence of long patient wires that can compromise the measures introducing noise source due to their movement.

In conclusion, the aim of this study was to propose a new measurement approach for the assessment of the diaphragmatic signal. The obtained results prove that this system works and is able to detect the diaphragm motion provoked by the respiratory cycle. This kind of approach could be a suitable technique to monitor the pathological patient that requires constant monitoring and it can be applied on the preterms babies with assisted ventilation to evaluate their diaphragmatic activity.

## 6. Acknowledgements

I would like to thank to my supervisor prof. Lorenzo Scalise for his useful critics and suggestions and for being a guide during my activity of internship.

I want to express my great appreciation to prof. Laura Falaschetti and prof. Giorgio Biagetti for helping me during the data acquisition and measurement session.

Finally, I want to thank to my co-supervisor Luca Antognoli for his support during all the internship activity, especially during the measurement sessions.

## List of Figures

Figure 1 - Bipolar modality sEMG acquisition [7].....	7
Figure 2 - Bipolar modality sEMG circuital representation [7].....	8
Figure 3 - Diaphragm .....	9
Figure 4 - Dipha-16 device [14].....	12
Figure 5- Electrode-skin interface [8] .....	14
Figure 6 - Electrode circuital representation [17].....	15
Figure 7 - Electrode prototype, PLA 3D Printing, Coating process [18] .....	18
Figure 8 - 3D Printed Electrode [19] .....	18
Figure 9 - Dry electrode [20] .....	19
Figure 10 - Adhesive gel patch .....	22
Figure 11 - Bare Conductive Electric Paint [23] .....	22
Figure 12 - Adhesive conductive electrode .....	23
Figure 13 - Adhesive conductive electrode-skin interface .....	24
Figure 14 - Mobile node block-scheme .....	26
Figure 15 - Mobile node composition .....	28
Figure 16 - Mobile node architecture.....	28
Figure 17 – Spirometer .....	30
Figure 18 - Adhesive conductive electrode positioning .....	32
Figure 19 - Correspondence between spirometer and raw EMG signal on subject LA .....	34
Figure 20 - Correspondence between spirometer and filtered EMG on subject LA .....	34
Figure 21 - Superimposition of Filtered, WT and Envelope EMG signal on subject LA .....	35
Figure 22 - Superimposition of PCA and Envelope EMG signal on subject LA .....	35
Figure 23 - Filtered EMG signal on subject LI.....	36
Figure 24 - Superimposition of Filtered, WT and Envelope EMG signal on subject LI .....	36

Figure 25 - Alternation of deep and normal breaths on subject LI.....	37
Figure 26 - Superimposition of PCA and Envelope EMG signal on subject LI.....	37
Figure 27 - Filtered EMG signal on subject SM .....	38
Figure 28 - Superimposition of Filtered, WT and Envelope EMG signal on subject SM .....	38
Figure 29 - Alternation of deep and normal breaths on subject SM .....	39
Figure 30 - Superimposition of PCA and Envelope EMG signal on subject SM .....	39
Figure 31 - Filtered EMG signal on subject SP.....	40
Figure 32 - Superimposition of Filtered, WT and Envelope EMG signal on subject SP .....	40
Figure 33 - Alternation of deep and normal breaths on subject SP.....	41
Figure 34 - Superimposition of PCA and Envelope EMG signal on subject SP .....	41
Figure 35 - Filtered EMG signal on subject MO .....	42
Figure 36 - Superimposition of Filtered, WT and Envelope EMG signal on subject MO .....	42
Figure 37 - Alternation of deep and normal breaths on subject MO .....	43
Figure 38 - Superimposition of PCA and Envelope EMG signal on subject MO .....	43
Figure 39 - Filtered EMG signal on subject AP .....	44
Figure 40 - Superimposition of Filtered, WT and Envelope EMG signal on subject AP .....	44
Figure 41 - Alternation of deep and normal breaths on subject AP .....	45
Figure 42 - Superimposition of PCA and Envelope EMG signal on subject AP .....	45
Figure 43 - Filtered EMG signal on subject MM.....	46
Figure 44 - Superimposition of Filtered, WT and Envelope EMG signal on subject MM .....	46
Figure 45 - Alternation of deep and normal breaths on subject MM .....	47
Figure 46 - Superimposition of PCA and Envelope EMG signal on subject MM ....	47
Figure 47 - Filtered EMG signal on subject AB .....	48
Figure 48 - Superimposition of Filtered, WT and Envelope EMG signal on subject AB .....	48

Figure 49 - Alternation of deep and normal breaths on subject AB .....	49
Figure 50 - Superimposition of PCA and Envelope EMG signal on subject AB.....	49
Figure 51 - Filtered EMG signal on subject AC .....	50
Figure 52 - Superimposition of Filtered, WT and Envelope EMG signal on subject AC .....	50
Figure 53 - Alternation of deep and normal breaths on subject AC.....	51
Figure 54 - Superimposition of PCA and Envelope EMG signal on subject AC.....	51
Figure 55 - Filtered EMG signal on subject MTP .....	52
Figure 56 - Superimposition of Filtered, WT and Envelope EMG signal on subject MTP .....	52
Figure 57 - Alternation of deep and normal breaths on subject MTP.....	53
Figure 58 - Superimposition of PCA and Envelope EMG signal on subject MTP....	53

## Bibliography

- [1] B.H. Brown, R.H. Smallwood, D.C. Barber, P.V. Lawford and D.R. Hose. *Medical Physics and Biomedical Engineering*. Medical Science Series, 1999.
- [2] C.L. Stanfield. *Principles of Human Physiology Fifth Edition*. Pearson, 2013.
- [3] P. Tallgren, S. Vanhatalo, K. Kaila, J. Voipio. *Evaluation of commercially available electrodes and gels for recording of slow EEG potentials*. *Clinical Neurophysiology* 116, 2005, (799–806).
- [4] A. Cappello, A. Cappozzo and P.E. di Prampero. *Bioingegneria della postura e del movimento*. Patron Editore, 2003.
- [5] Motion Lab Systems. *EMG Analysis, A software user guide for EMG Graphing and EMG Analysis*. Motion Lab Systems Inc. February 2009.
- [6] C.J. DeLuca, L.D. Gilmore, M. Kuznetsov, S. H. Roy. *Filtering the surface EMG signal: Movement artifact and baseline noise contamination*. *Journal of Biomechanics*, January 2010.
- [7] D.F. Stageman, H.J. Hermens. *Standards for surface electromyography: The European project Surface EMG for non-invasive assessment of muscles (SENIAM)*. January 2007.
- [8] V.L. da Silveira Nantes Button. *Principles of Measurement and Transduction of Biomedical Variables*. Elsevier, 2015.
- [9] T. Elenbaas. *Breath detection by diaphragm electromyography in neonates*. Eindhoven University of Technology, 2000.
- [10] L. Estrada, A.Torres , L. Sarlabous and R. Jan´e. *Onset and Offset Estimation of the Neural Inspiratory Time in Surface Diaphragm Electromyography: A Pilot Study in Healthy Subjects*. *IEEE Journal of Biomedical and health informatics*, January 2018.
- [11] S.R. Alty, W.D.C. Man, J. Moxham and K.C. Lee. *Denoising of Diaphragmatic Electromyogram Signals for Respiratory Control and Diagnostic Purposes*. 30th

Annual International IEEE EMBS Conference Vancouver, British Columbia, Canada, August 20-24, 2008.

[12] R.W. van Leuteren, G.J. Hutten, C.G. de Waal, P. Dixon, A.H. van Kaam, F.H. de Jongh. *Processing transcutaneous electromyography measurements of respiratory muscles, a review of analysis techniques*. Journal of Electromyography and Kinesiology, 2019 (176-186).

[13] I.M. Masselli Dos Reis, D.G. Ohara, L. Bergamin Januario, R. Pedrolongo Basso-Vanelli, A.B.Oliveira, M. Jamami. *Surface electromyography in inspiratory muscles in adults and elderly individuals: A systematic review*. Journal of Electromyography and Kinesiology, 2019 (139-155).

[14] Demcom Macawi Respiratory system. *USER MANUAL Instruction for use Dipher Application program*.

[15] L.C. Yia, O.A. Nascimento, J.R. Jardim. *Reliability of an Analysis Method for Measuring Diaphragm Excursion by Means of Direct Visualization with Videofluoroscopy*. Arch Bronconeumol. 2011;47(6):310–314.

[16] H. Sumbul, A. H. Yuzer. *Measuring of Diaphragm Movements by using iMEMS Acceleration Sensor*. 9th International Conference on Electrical and Electronics Engineering (ELECO), 2015.

[17] F.P. Branca. *Fondamenti di Ingegneria Clinica Volume 1*. Springer

[18] S. Krachunov, A. J. Casson. *3D Printed Dry EEG Electrodes*. Sensors, October 2016.

[19] G. Wolterink, R. Sanders, F. Muijzer, B. van Beijnum, G. Krijnen. *3D-Printing Soft sEMG Sensing Structures*. IEEE, 2017.

[20] P. Salvo, R. Raedt, E. Carrette, D. Schaubroeck, J. Vanfleteren, L. Cardon. *A 3D Printed Dry Electrode for ECG/EEG Recording*. Sensors and Actuators A 174, 2012, (96– 102).

[21] C. Wang, K. Xia, H. Wang, X. Liang, Z. Yin, and Y. Zhang. *Advanced Carbon for Flexible and Wearable Electronics*. Adv. Mater. 2019, 31, 1801072.

[22] S.K.H. Gulrez, S. Al-Assaf and G. O Phillips. *Hydrogels: Methods of Preparation*,

*Characterisation and Applications.* www.intechopen.com

[23] [https://www.bareconductive.com/wpcontent/uploads/2015/01/MSDS\\_BareConductive\\_ElectricPaint.pdf](https://www.bareconductive.com/wpcontent/uploads/2015/01/MSDS_BareConductive_ElectricPaint.pdf)

[24] G. Biagetti, P. Crippa, L. Falaschetti, S. Orcioni, C. Turchetti. Wireless Surface Electromyograph and Electrocardiograph System on 802.15.4. IEEE Transactions on Consumer Electronics, Vol. 62, No. 3, August 2016.

[25] [https://infocenter.nordicsemi.com/pdf/nRF52840\\_PS\\_v1.0.pdf](https://infocenter.nordicsemi.com/pdf/nRF52840_PS_v1.0.pdf)

[26] <http://www.ti.com/lit/ds/symlink/ads1293.pdf>

[27] <https://www.st.com/resource/en/datasheet/lsm6dso.pdf>

[28] J. Kilby, H.G. Hosseini. *Wavelet Analysis of Surface Electromyography Signals*. Proceedings of the 26th Annual International Conference of the IEEE EMBS San Francisco, CA, USA September 1-5, 2004.

[29] S. Abbaspour M. Linden H.G. Hosseini. *ECG Artifact Removal from Surface EMG Signal Using an Automated Method Based on Wavelet-ICA*. 12th International Conference on Wearable Micro and Nano Technologies for Personalized Health, At Sweden, June 2015.

[30] I.T. Jolliffe. *Principal Component Analysis*. Springer 2002.

[31] A.D. Valentine, T.A. Busbee, J.W. Boley, J.R. Raney, A. Chortos, A. Kotikian, J. D. Berrigan, M. F. Durstock, and J.A. Lewis. *Hybrid 3D Printing of Soft Electronics*. Adv. Mater. 29, 1703817, 2017.